Chapter 1

Non-linear Surface Susceptibility

In this section we outline the general procedure to obtain the surface susceptibility tensor for second harmonic generation. We start with the non-linear polarization $\mathbf{P}$ written as

$$\begin{aligned} P_{\mathrm{a}}(2\omega) = \chi_{\mathrm{abc}}(-2\omega;\omega,\omega)E_{\mathrm{b}}(\omega)E_{\mathrm{c}}(\omega) \\ + \chi_{\mathrm{abcl}}(-2\omega;\omega,\omega)E_{\mathrm{b}}(\omega)\nabla_{\mathrm{c}}E_{\mathrm{l}}(\omega) + \cdots , \end{aligned} \tag{1.1}$$

where $\chi_{\mathrm{abc}}(-2\omega;\omega,\omega)$ and $\chi_{\mathrm{abcl}}(-2\omega;\omega,\omega)$ correspond to the dipolar and quadrupolar susceptibilities. We drop the $(-2\omega;\omega,\omega)$ argument to ease on the notation. The sum continues with higher multipolar terms. If we consider a semi-infinite system with a centrosymmetric bulk, the equation above can be separated into two contributions from symmetry considerations alone; one from the surface of the system and the other from the bulk of the system. We take

$$P_{\mathrm{a}}(\mathbf{r}) = \chi_{\mathrm{abc}}E_{\mathrm{b}}(\mathbf{r})E_{\mathrm{c}}(\mathbf{r}) + \chi_{\mathrm{abcl}}E_{\mathrm{b}}(\mathbf{r})\frac{\partial}{\partial \mathbf{r}_{\mathrm{c}}}E_{\mathrm{l}}(\mathbf{r}) + \cdots , \tag{1.2}$$

as the polarization with respect to the original coordinate system, and

$$\begin{aligned} P_{\mathrm{a}}(-\mathbf{r}) = \chi_{\mathrm{abc}}E_{\mathrm{b}}(-\mathbf{r})E_{\mathrm{c}}(-\mathbf{r}) \\ + \chi_{\mathrm{abcl}}E_{\mathrm{b}}(-\mathbf{r})\frac{\partial}{\partial(-\mathbf{r}_{\mathrm{c}})}E_{\mathrm{l}}(-\mathbf{r}) + \cdots , \end{aligned} \tag{1.3}$$

as the polarization in the coordinate system where inversion is taken, i.e. $\mathbf{r} \to -\mathbf{r}$. Note that we have kept the same susceptibility tensors, and they must be invariant under $\mathbf{r} \to -\mathbf{r}$ since the system is centrosymmetric. Recalling that $\mathbf{P}(\mathbf{r})$ and $\mathbf{E}(\mathbf{r})$ are polar vectors [**?**], we have that Eq. (1.3) reduces to

$$\begin{aligned} -P_{\mathrm{a}}(\mathbf{r}) = \chi_{\mathrm{abc}}(-E_{\mathrm{b}}(\mathbf{r}))(-E_{\mathrm{c}}(\mathbf{r})) - \chi_{\mathrm{abcl}}(-E_{\mathrm{b}}(\mathbf{r}))(-\frac{\partial}{\partial \mathbf{r}_{\mathrm{c}}})(-E_{\mathrm{l}}(\mathbf{r})) + \cdots , \\ P_{\mathrm{a}}(\mathbf{r}) = -\chi_{\mathrm{abc}}E_{\mathrm{b}}(\mathbf{r})E_{\mathrm{c}}(\mathbf{r}) + \chi_{\mathrm{abcl}}E_{\mathrm{b}}(\mathbf{r})\frac{\partial}{\partial \mathbf{r}_{\mathrm{c}}}E_{\mathrm{l}}(\mathbf{r}) + \cdots , \end{aligned} \tag{1.4}$$

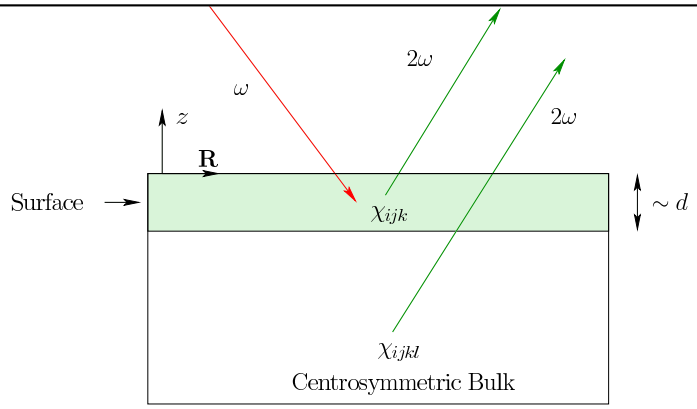

Figure 1.1: (Color Online) Sketch of the semi-infinite system with a centrosymmetric bulk. The surface region is of width $\sim d$. The incoming photon of frequency ω is represented by a downward red arrow, whereas both the surface and bulk created second harmonic photons of frequency 2ω are represented by upward green arrows. The red color suggests an incoming infrared photon with a green second harmonic photon. The dipolar ($\chi_{\rm abc}$), and quadrupolar ($\chi_{\rm abcl}$) susceptibility tensors are shown in the regions where they are different from zero. The axis has z perpendicular to the surface and $\mathbf{R}$ parallel to it.

that when compared with Eq. (1.2) leads to the conclusion that

$$\chi_{\rm abc} = 0 \tag{1.5}$$

for a centrosymmetric bulk.

If we move to the surface of the semi-infinite system our assumption of centrosymmetry breaks down, and there is no restriction in $\chi_{\rm abc}$. We conclude that the leading term of the polarization in a surface region is given by

$$\int dz P_{\rm a}(\mathbf{R}, z) \approx d P_{\rm a} \equiv P^S_{\rm a} \equiv \chi^S_{\rm abc} E_{\rm b} E_{\rm c}, \tag{1.6}$$

where d is the surface region from which the dipolar signal of $\mathbf{P}$ is different from zero (see Fig. 1.1), and $\mathbf{P}^S \equiv d\mathbf{P}$ is the surface SH polarization. Then, from Eq. (1.1) we obtain that

$$\chi^S_{\rm abc} = d\chi_{\rm abc} \tag{1.7}$$

is the SH surface susceptibility. On the other hand,

$$P^b_{\rm a}(\mathbf{r}) = \chi_{\rm abcl} E_{\rm b}(\mathbf{r}) \nabla_{\rm c} E_{\rm l}(\mathbf{r}), \tag{1.8}$$

gives the bulk polarization. We immediately recognize that the surface polarization is of dipolar order while the bulk polarization is of quadrupolar order. The surface, $\chi^S_{\rm abc}$, and bulk, $\chi_{\rm abcl}$, susceptibility tensor ranks are three and four, respectively. We will only concentrate on surface SHG in this article even though bulk generated SH is also a very important optical phenomenon. Also, we leave out of this article other interesting surface SH phenomena like, electric field induced second harmonic (EFISH), which would be represented by a surface susceptibility tensor of quadrupolar origin. In centrosymmetric systems for which the quadrupolar bulk response is much smaller than the dipolar surface response, SH is readily used as a very useful and powerful optical surface probe.[1]

In the following sections we present the theoretical approach to derive the expressions for the surface susceptibility tensor $\chi^S_{\rm abc}$.

1.1 Length Gauge

We follow the article by Aversa and Sipe[2] to calculate the optical properties of a given system within the longitudinal gauge. More recent derivations can also be found in Refs. [3, 4]. Assuming the long-wavelength approximation which implies a position independent electric field, $\mathbf{E}(t)$, the Hamiltonian in the length gauge approximation is given by

$$\hat{H} = \hat{H}^\sigma_0 - e\hat{\mathbf{r}} \cdot \mathbf{E}, \tag{1.9}$$

with

$$\hat{H}^\sigma_0 = \hat{H}^{\rm LDA}_0 + \mathcal{S}(\mathbf{r}, \mathbf{p}), \tag{1.10}$$

as the unperturbed Hamiltonian. The LDA Hamiltonian can be expressed as follows,

$$\begin{aligned} \hat{H}^{\rm LDA}_0 &= \frac{\hat{p}^2}{2m_e} + \hat{V}^{\rm ps} \\ \hat{V}^{\rm ps} &= \hat{V}^l(\hat{\mathbf{r}}) + \hat{V}^{\rm nl}, \end{aligned} \tag{1.11}$$

where $\hat{V}^l(\hat{\mathbf{r}})$ and $\hat{V}^{\rm nl}$ are the local and the non-local parts of the crystal pseudopotential $\hat{V}^{\rm ps}$. For the latter, we have that

$$V^{\rm nl}(\mathbf{r}, \mathbf{r}') \equiv \langle \mathbf{r} | \hat{V}^{\rm nl} | \mathbf{r}' \rangle \neq 0 \quad \text{for} \quad \mathbf{r} \neq \mathbf{r}', \tag{1.12}$$

where $V^{\rm nl}(\mathbf{r},\mathbf{r}')$ is a function of $\mathbf{r}$ and $\mathbf{r}'$ representing the non-local contribution of the pseudopotential. The Schrödinger equation reads

$$\left(\frac{-\hbar^2}{2m_e}\nabla^2+\hat{V}^l(\mathbf{r})\right)\psi_{n\mathbf{k}}(\mathbf{r})+\int d\mathbf{r}'\hat{V}^{\rm nl}(\mathbf{r},\mathbf{r}')\psi_{n\mathbf{k}}(\mathbf{r}')=E_i\psi_{n\mathbf{k}}(\mathbf{r}), \quad (1.13)$$

where $\psi_{n\mathbf{k}}(\mathbf{r})=\langle\mathbf{r}|n\mathbf{k}\rangle=e^{i\mathbf{k}\cdot\mathbf{r}}u_{n\mathbf{k}}(\mathbf{r})$, are the real space representations of the Bloch states $|n\mathbf{k}\rangle$ labelled by the band index n and the crystal momentum $\mathbf{k}$, and $u_{n\mathbf{k}}(\mathbf{r})$ is cell periodic. m_e is the bare mass of the electron and Ω is the unit cell volume. The nonlocal scissors operator is given by

$$\mathcal{S}(\mathbf{r},\mathbf{p})=\hbar\Sigma\sum_n\int d^3k'(1-f_n(\mathbf{k}))|n\mathbf{k}'\rangle\langle n\mathbf{k}'|, \quad (1.14)$$

where $f_n(\mathbf{k})$ is the occupation number, that for $T=0$ K, is independent of $\mathbf{k}$, and is one for filled bands and zero for unoccupied bands. For semiconductors the filled bands correspond to valence bands ($n=v$) and the unoccupied bands to conduction bands ($n=c$). We have that

$$\begin{aligned} H_0^{\rm LDA}|n\mathbf{k}\rangle&=\hbar\omega_n^{\rm LDA}(\mathbf{k})|n\mathbf{k}\rangle \\ H_0^{\sigma}|n\mathbf{k}\rangle&=\hbar\omega_n^{\sigma}(\mathbf{k})|n\mathbf{k}\rangle, \end{aligned} \quad (1.15)$$

where

$$\hbar\omega_n^{\sigma}(\mathbf{k})=\hbar\omega_n^{\rm LDA}(\mathbf{k})+\hbar\Sigma(1-f_n), \quad (1.16)$$

is the scissored energy. Here, $\hbar\Sigma$ is the value by which the conduction bands are rigidly ($\mathbf{k}$-independent) shifted upwards in energy, also known as the scissors shift. Σ could be taken to be $\mathbf{k}$ dependent, but for most calculations (like the ones presented here), a rigid shift is sufficient. We can take $\hbar\Sigma=E_g-E_g^{\rm LDA}$ where E_g could be the experimental band gap or GW band gap taken at the Γ point, i.e. $\mathbf{k}=0$. We used the fact that $|n\mathbf{k}\rangle^{\rm LDA}\approx|n\mathbf{k}\rangle^{\sigma}$, thus negating the need to label the Bloch states with the LDA or σ superscripts. The matrix elements of $\mathbf{r}$ are split between the *intraband* ($\mathbf{r}_i$) and *interband* ($\mathbf{r}_e$) parts , where $\mathbf{r}=\mathbf{r}_i+\mathbf{r}_e$ and [5, 6, 2]

$$\langle n\mathbf{k}|\hat{\mathbf{r}}_i|m\mathbf{k}'\rangle=\delta_{nm}\left[\delta(\mathbf{k}-\mathbf{k}')\boldsymbol{\xi}_{nn}(\mathbf{k})+i\nabla_{\mathbf{k}}\delta(\mathbf{k}-\mathbf{k}')\right], \quad (1.17)$$

$$\langle n\mathbf{k}|\hat{\mathbf{r}}_e|m\mathbf{k}'\rangle=(1-\delta_{nm})\delta(\mathbf{k}-\mathbf{k}')\boldsymbol{\xi}_{nm}(\mathbf{k}), \quad (1.18)$$

and

$$\boldsymbol{\xi}_{nm}(\mathbf{k})\equiv i\frac{(2\pi)^3}{\Omega}\int_\Omega d\mathbf{r}\,u_{n\mathbf{k}}^*(\mathbf{r})\nabla_{\mathbf{k}}u_{m\mathbf{k}}(\mathbf{r}). \quad (1.19)$$

The interband part $\mathbf{r}_e$ can be obtained as follows. We start by introducing the velocity operator

$$\hat{\mathbf{v}}^\sigma = \frac{1}{i\hbar}[\hat{\mathbf{r}}, \hat{H}_0^\sigma], \tag{1.20}$$

and calculating its matrix elements

$$i\hbar\langle n\mathbf{k}|\mathbf{v}^\sigma|m\mathbf{k}\rangle = \langle n\mathbf{k}|[\hat{\mathbf{r}}, \hat{H}_0^\sigma]|m\mathbf{k}\rangle = \langle n\mathbf{k}|\hat{\mathbf{r}}\hat{H}_0^\sigma - \hat{H}_0^\sigma\hat{\mathbf{r}}|m\mathbf{k}\rangle = (\hbar\omega_m^\sigma(\mathbf{k}) - \hbar\omega_n^\sigma(\mathbf{k}))\langle n\mathbf{k}|\hat{\mathbf{r}}|m\mathbf{k}\rangle, \tag{1.21}$$

thus defining $\omega_{nm}^\sigma(\mathbf{k}) = \omega_n^\sigma(\mathbf{k}) - \omega_m^\sigma(\mathbf{k})$ we get

$$\mathbf{r}_{nm}(\mathbf{k}) = \frac{\mathbf{v}_{nm}^\sigma(\mathbf{k})}{i\omega_{nm}^\sigma(\mathbf{k})} \qquad n \notin D_m, \tag{1.22}$$

which can be identified as $\mathbf{r}_{nm} = (1 - \delta_{nm})\boldsymbol{\xi}_{nm} \to \mathbf{r}_{e,nm}$. Here, D_m are all the possible degenerate m-states. When $\mathbf{r}_i$ appears in commutators we use[2]

$$\langle n\mathbf{k}|[\hat{\mathbf{r}}_i, \hat{\mathcal{O}}]|m\mathbf{k}'\rangle = i\delta(\mathbf{k} - \mathbf{k}')(\mathcal{O}_{nm})_{;\mathbf{k}}, \tag{1.23}$$

with

$$(\mathcal{O}_{nm})_{;\mathbf{k}} = \nabla_{\mathbf{k}}\mathcal{O}_{nm}(\mathbf{k}) - i\mathcal{O}_{nm}(\mathbf{k})\left(\boldsymbol{\xi}_{nn}(\mathbf{k}) - \boldsymbol{\xi}_{mm}(\mathbf{k})\right), \tag{1.24}$$

where "$;\mathbf{k}$" denotes the generalized derivative (see Appendix **??**).

As can be seen from Eq. (1.10) and (1.11), both $\hat{S}$ and $\hat{V}^{\rm nl}$ are nonlocal potentials. Their contribution in the calculation of the optical response has to be taken in order to get reliable results.[7] We proceed as follows; from Eqs. (1.20), (1.10) and (1.11) we find

$$\begin{aligned}\hat{\mathbf{v}}^\sigma &= \frac{\hat{\mathbf{p}}}{m_e} + \frac{1}{i\hbar}[\hat{\mathbf{r}}, \hat{V}^{\rm nl}(\mathbf{r}, \mathbf{r}')] + \frac{1}{i\hbar}[\hat{\mathbf{r}}, \hat{\mathcal{S}}(\mathbf{r}, \mathbf{p})] \\ &\equiv \hat{\mathbf{v}} + \hat{\mathbf{v}}^{\rm nl} + \hat{\mathbf{v}}^{\mathcal{S}} = \hat{\mathbf{v}}^{\rm LDA} + \hat{\mathbf{v}}^{\mathcal{S}},\end{aligned} \tag{1.25}$$

where we have defined

$$\begin{aligned}\hat{\mathbf{v}} &= \frac{\hat{\mathbf{p}}}{m_e} \\ \hat{\mathbf{v}}^{\rm nl} &= \frac{1}{i\hbar}[\hat{\mathbf{r}}, \hat{V}^{\rm nl}] \\ \hat{\mathbf{v}}^{\mathcal{S}} &= \frac{1}{i\hbar}[\hat{\mathbf{r}}, \hat{S}(\mathbf{r}, \mathbf{p})] \\ \hat{\mathbf{v}}^{\rm LDA} &= \hat{\mathbf{v}} + \hat{\mathbf{v}}^{\rm nl}\end{aligned} \tag{1.26}$$

with $\hat{\mathbf{p}} = -i\hbar\boldsymbol{\nabla}$ the momentum operator. Using Eq. (1.14), we obtain that the matrix elements of $\hat{\mathbf{v}}^{\mathcal{S}}$ are given by

$$\mathbf{v}^{\mathcal{S}}_{nm} = i\Sigma f_{mn}\mathbf{r}_{nm}, \tag{1.27}$$

with $f_{nm} = f_n - f_m$, where we see that $\mathbf{v}^{\mathcal{S}}_{nn} = 0$, then

$$\begin{aligned}
\mathbf{v}^{\sigma}_{nm} &= \mathbf{v}^{\mathrm{LDA}}_{nm} + i\Sigma f_{mn}\mathbf{r}_{nm} \\
&= \mathbf{v}^{\mathrm{LDA}}_{nm} + i\Sigma f_{mn}\frac{\mathbf{v}^{\sigma}_{nm}(\mathbf{k})}{i\omega^{\sigma}_{nm}(\mathbf{k})} \\
\mathbf{v}^{\sigma}_{nm}\frac{\omega^{\sigma}_{nm} - \Sigma f_{mn}}{\omega^{\sigma}_{nm}} &= \mathbf{v}^{\mathrm{LDA}}_{nm} \\
\mathbf{v}^{\sigma}_{nm}\frac{\omega^{\mathrm{LDA}}_{nm}}{\omega^{\sigma}_{nm}} &= \mathbf{v}^{\mathrm{LDA}}_{nm} \\
\frac{\mathbf{v}^{\sigma}_{nm}}{\omega^{\sigma}_{nm}} &= \frac{\mathbf{v}^{\mathrm{LDA}}_{nm}}{\omega^{\mathrm{LDA}}_{nm}},
\end{aligned} \tag{1.28}$$

since $\omega^{\sigma}_{nm} - \Sigma f_{mn} = \omega^{\mathrm{LDA}}_{nm}$. Therefore,

$$\begin{aligned}
\mathbf{v}^{\sigma}_{nm}(\mathbf{k}) &= \frac{\omega^{\sigma}_{nm}}{\omega^{\mathrm{LDA}}_{nm}}\mathbf{v}^{\mathrm{LDA}}_{nm}(\mathbf{k}) = \left(1 + \frac{\Sigma}{\omega_c(\mathbf{k}) - \omega_v(\mathbf{k})}\right)\mathbf{v}^{\mathrm{LDA}}_{nm}(\mathbf{k}) \qquad n \notin D_m \\
\mathbf{v}^{\sigma}_{nn}(\mathbf{k}) &= \mathbf{v}^{\mathrm{LDA}}_{nn}(\mathbf{k}),
\end{aligned} \tag{1.29}$$

and Eq. (1.22) gives

$$\mathbf{r}_{nm}(\mathbf{k}) = \frac{\mathbf{v}^{\sigma}_{nm}(\mathbf{k})}{i\omega^{\sigma}_{nm}(\mathbf{k})} = \frac{\mathbf{v}^{\mathrm{LDA}}_{nm}(\mathbf{k})}{i\omega^{\mathrm{LDA}}_{nm}(\mathbf{k})} \qquad n \notin D_m. \tag{1.30}$$

The matrix elements of $\mathbf{r}_e$ are the same whether we use the LDA or the scissored Hamiltonian and there is no need to label them with either LDA or S superscripts. Thus, we can write

$$\mathbf{r}_{e,nm} \to \mathbf{r}_{nm}(\mathbf{k}) = \frac{\mathbf{v}^{\mathrm{LDA}}_{nm}(\mathbf{k})}{i\omega^{\mathrm{LDA}}_{nm}(\mathbf{k})} \qquad n \notin D_m, \tag{1.31}$$

which gives the interband matrix elements of the position operator in terms of the matrix elements of $\hat{\mathbf{v}}^{\mathrm{LDA}}$. These matrix elements include the matrix elements of $\mathbf{v}^{\mathrm{nl}}_{nm}(\mathbf{k})$ which can be readily calculated[**?**] for fully separable nonlocal pseudopotentials in the Kleinman-Bylander form.[8, 9, 10] In Appendix **??** we outline how this can be accomplished.

1.2 Time-dependent Perturbation Theory

In the independent particle approximation, we use the electron density operator $\hat{\rho}$ to obtain the expectation value of any observable $\mathcal{O}$ as

$$\mathcal{O} = \mathrm{Tr}(\hat{\mathcal{O}}\hat{\rho}) = \mathrm{Tr}(\hat{\rho}\hat{\mathcal{O}}), \tag{1.32}$$

where Tr is the trace and is invariant under cyclic permutations. The dynamic equation of motion for ρ is given by

$$i\hbar\frac{d\hat{\rho}}{dt} = [\hat{H}, \hat{\rho}], \tag{1.33}$$

where it is more convenient to work in the interaction picture. We transform all operators according to

$$\hat{\mathcal{O}}_I = \hat{U}\hat{\mathcal{O}}\hat{U}^\dagger, \tag{1.34}$$

where

$$\hat{U} = e^{i\hat{H}_0 t/\hbar}, \tag{1.35}$$

is the unitary operator that shifts us to the interaction picture. Note that $\hat{\mathcal{O}}_I$ depends on time even if $\hat{\mathcal{O}}$ does not. Then, we transform Eq. (1.33) into

$$i\hbar\frac{d\hat{\rho}_I(t)}{dt} = [-e\hat{\mathbf{r}}_I(t)\cdot\mathbf{E}(t), \hat{\rho}_I(t)], \tag{1.36}$$

that leads to

$$\hat{\rho}_I(t) = \hat{\rho}_I(t=-\infty) + \frac{ie}{\hbar}\int_{-\infty}^{t} dt'[\hat{\mathbf{r}}_I(t')\cdot\mathbf{E}(t'), \hat{\rho}_I(t')]. \tag{1.37}$$

We assume that the interaction is switched-on adiabatically and choose a time-periodic perturbing field, to write

$$\mathbf{E}(t) = \mathbf{E}e^{-i\omega t}e^{\eta t} = \mathbf{E}e^{-i\tilde{\omega}t}, \tag{1.38}$$

with

$$\tilde{\omega} = \omega + i\eta, \tag{1.39}$$

where $\eta > 0$ assures that at $t = -\infty$ the interaction is zero and has its full strength $\mathbf{E}$ at $t = 0$. After computing the required time integrals one takes $\eta \to 0$. Also, $\hat{\rho}_I(t=-\infty)$ should be time independent and thus $[\hat{H}, \hat{\rho}]_{t=-\infty} = 0$, This implies that $\hat{\rho}_I(t=-\infty) = \hat{\rho}(t=-\infty) \equiv \hat{\rho}_0$, where $\hat{\rho}_0$ is the density matrix of the unperturbed ground state, such that

$$\langle n\mathbf{k}|\hat{\rho}_0|m\mathbf{k}'\rangle = f_n(\hbar\omega_n^\sigma(\mathbf{k}))\delta_{nm}\delta(\mathbf{k}-\mathbf{k}'), \tag{1.40}$$

with $f_n(\hbar\omega_n^\sigma(\mathbf{k})) = f_{n\mathbf{k}}$ as the Fermi-Dirac distribution function.

We solve Eq. (1.37) using the standard iterative solution, for which we write

$$\hat{\rho}_I = \hat{\rho}_I^{(0)} + \hat{\rho}_I^{(1)} + \hat{\rho}_I^{(2)} + \cdots, \tag{1.41}$$

where $\hat{\rho}_I^{(N)}$ is the density operator to order N in $\mathbf{E}(t)$. Then, Eq. (1.37) reads

$$\hat{\rho}_I^{(0)} + \hat{\rho}_I^{(1)} + \hat{\rho}_I^{(2)} + \cdots = \hat{\rho}_0 + \frac{ie}{\hbar}\int_{-\infty}^{t} dt'[\hat{\mathbf{r}}_I(t')\cdot\mathbf{E}(t'), \hat{\rho}_I^{(0)} + \hat{\rho}_I^{(1)} + \hat{\rho}_I^{(2)} + \cdots], \tag{1.42}$$

where, by equating equal orders in the perturbation, we find

$$\hat{\rho}_I^{(0)} \equiv \hat{\rho}_0, \tag{1.43}$$

and

$$\hat{\rho}_I^{(N)}(t) = \frac{ie}{\hbar}\int_{-\infty}^{t} dt'[\hat{\mathbf{r}}_I(t')\cdot\mathbf{E}(t'), \hat{\rho}_I^{(N-1)}(t')]. \tag{1.44}$$

It is simple to show that matrix elements of Eq. (1.44) satisfy $\langle n\mathbf{k}|\rho_I^{(N+1)}(t)|m\mathbf{k}'\rangle = \rho_{I,nm}^{(N+1)}(\mathbf{k})\delta(\mathbf{k}-\mathbf{k}')$, with

$$\rho_{I,nm}^{(N+1)}(\mathbf{k};t) = \frac{ie}{\hbar}\int_{-\infty}^{t} dt'\langle n\mathbf{k}|[\hat{\mathbf{r}}_I(t'), \hat{\rho}_I^{(N)}(t')]|m\mathbf{k}\rangle\cdot\mathbf{E}(t'). \tag{1.45}$$

We now work out the commutator of Eq. (1.45). Then,

$$\begin{aligned}\langle n\mathbf{k}|[\hat{\mathbf{r}}_I(t), \hat{\rho}_I^{(N)}(t)]|m\mathbf{k}\rangle &= \langle n\mathbf{k}|[\hat{U}\hat{\mathbf{r}}\hat{U}^\dagger, \hat{U}\hat{\rho}^{(N)}(t)\hat{U}^\dagger]|m\mathbf{k}\rangle \\ &= \langle n\mathbf{k}|\hat{U}[\hat{\mathbf{r}}, \hat{\rho}^{(N)}(t)]\hat{U}^\dagger|m\mathbf{k}\rangle \\ &= e^{i\omega_{nm\mathbf{k}}^\sigma t}\left(\langle n\mathbf{k}|[\hat{\mathbf{r}}_e, \hat{\rho}^{(N)}(t)] + [\hat{\mathbf{r}}_i, \hat{\rho}^{(N)}(t)]|m\mathbf{k}\rangle\right).\end{aligned} \tag{1.46}$$

We calculate the interband term first, so using Eq. (1.31) we obtain

$$\begin{aligned}\langle n\mathbf{k}|[\hat{\mathbf{r}}_e, \hat{\rho}^{(N)}(t)]|m\mathbf{k}\rangle &= \sum_\ell \Big(\langle n\mathbf{k}|\hat{\mathbf{r}}_e|\ell\mathbf{k}\rangle\langle\ell\mathbf{k}|\hat{\rho}^{(N)}(t)|m\mathbf{k}\rangle \\ &\quad -\langle n\mathbf{k}|\hat{\rho}^{(N)}(t)|\ell\mathbf{k}\rangle\langle\ell\mathbf{k}|\hat{\mathbf{r}}_e|m\mathbf{k}\rangle\Big) \\ &= \sum_{\ell\neq n,m}\Big(\mathbf{r}_{n\ell}(\mathbf{k})\rho_{\ell m}^{(N)}(\mathbf{k};t) - \rho_{n\ell}^{(N)}(\mathbf{k};t)\mathbf{r}_{\ell m}(\mathbf{k})\Big) \\ &\equiv \mathbf{R}_e^{(N)}(\mathbf{k};t),\end{aligned} \tag{1.47}$$

and from Eq. (1.23),

$$\langle n\mathbf{k}|[\hat{\mathbf{r}}_i, \hat{\rho}^{(N)}(t)]|m\mathbf{k}'\rangle = i\delta(\mathbf{k}-\mathbf{k}')(\rho^{(N)}_{nm}(t))_{;\mathbf{k}} \equiv \delta(\mathbf{k}-\mathbf{k}')\mathbf{R}^{(N)}_i(\mathbf{k};t). \quad (1.48)$$

Then Eq. (1.45) becomes

$$\rho^{(N+1)}_{I,nm}(\mathbf{k};t) = \frac{ie}{\hbar}\int_{-\infty}^{t} dt' e^{i(\omega^{\sigma}_{nm\mathbf{k}}-\tilde{\omega})t'}\left[R^{\mathrm{b}(N)}_e(\mathbf{k};t') + R^{\mathrm{b}(N)}_i(\mathbf{k};t')\right]E^{\mathrm{b}}, \quad (1.49)$$

where the roman superindices a, b, c denote Cartesian components that are summed over if repeated. Starting from the linear response and proceeding from Eq. (1.40) and (1.47),

$$\begin{aligned} R^{\mathrm{b}(0)}_e(\mathbf{k};t) &= \sum_{\ell}\left(r^{\mathrm{b}}_{n\ell}(\mathbf{k})\rho^{(0)}_{\ell m}(\mathbf{k}) - \rho^{(0)}_{n\ell}(\mathbf{k})r^{\mathrm{b}}_{\ell m}(\mathbf{k})\right) \\ &= \sum_{\ell}\left(r^{\mathrm{b}}_{n\ell}(\mathbf{k})\delta_{\ell m}f_m(\hbar\omega^{\sigma}_m(\mathbf{k})) - \delta_{n\ell}f_n(\hbar\omega^{\sigma}_n(\mathbf{k}))r^{\mathrm{b}}_{\ell m}(\mathbf{k})\right) \\ &= f_{mn\mathbf{k}}r^{\mathrm{b}}_{nm}(\mathbf{k}), \end{aligned} \quad (1.50)$$

where $f_{mn\mathbf{k}} = f_{m\mathbf{k}} - f_{n\mathbf{k}}$. From now on, it should be clear that the matrix elements of $\mathbf{r}_{nm}$ imply $n \notin D_m$. We also have from Eq. (1.48) and Eq. (1.24) that

$$R^{\mathrm{b}(0)}_i(\mathbf{k}) = i(\rho^{(0)}_{nm})_{;k^{\mathrm{b}}} = i\delta_{nm}(f_{n\mathbf{k}})_{;k^{\mathrm{b}}} = i\delta_{nm}\nabla_{k^{\mathrm{b}}}f_{n\mathbf{k}}. \quad (1.51)$$

For a semiconductor at $T = 0$, $f_{n\mathbf{k}}$ is one if the state $|n\mathbf{k}\rangle$ is a valence state and zero if it is a conduction state; thus $\nabla_{\mathbf{k}}f_{n\mathbf{k}} = 0$ and $\mathbf{R}^{(0)}_i = 0$ and the linear response has no contribution from intraband transitions. Then,

$$\begin{aligned} \rho^{(1)}_{I,nm}(\mathbf{k};t) &= \frac{ie}{\hbar}f_{mn\mathbf{k}}r^{\mathrm{b}}_{nm}(\mathbf{k})E^{\mathrm{b}}\int_{-\infty}^{t} dt' e^{i(\omega^{\sigma}_{nm\mathbf{k}}-\tilde{\omega})t'} \\ &= \frac{e}{\hbar}f_{mn\mathbf{k}}r^{\mathrm{b}}_{nm}(\mathbf{k})E^{\mathrm{b}}\frac{e^{i(\omega^{\sigma}_{nm\mathbf{k}}-\tilde{\omega})t}}{\omega^{\sigma}_{nm\mathbf{k}}-\tilde{\omega}} \\ &= e^{i\omega^{\sigma}_{nm\mathbf{k}}t}B^{\mathrm{b}}_{mn}(\mathbf{k})E^{\mathrm{b}}(t) \\ &= e^{i\omega^{\sigma}_{nm\mathbf{k}}t}\rho^{(1)}_{nm}(\mathbf{k};t), \end{aligned} \quad (1.52)$$

with

$$B^{\mathrm{b}}_{nm}(\mathbf{k},\omega) = \frac{e}{\hbar}\frac{f_{mn\mathbf{k}}r^{\mathrm{b}}_{nm}(\mathbf{k})}{\omega^{\sigma}_{nm\mathbf{k}}-\tilde{\omega}}, \quad (1.53)$$

and

$$\rho^{(1)}_{nm}(\mathbf{k};t) = B^{\mathrm{b}}_{mn}(\mathbf{k},\omega)E^{\mathrm{b}}(\omega)e^{-i\tilde{\omega}t}. \quad (1.54)$$

Now, we calculate the second-order response. Then, from Eq. (1.47)

$$R_e^{\mathrm{b}(1)}(\mathbf{k};t) = \sum_\ell \left(r^{\mathrm{b}}_{n\ell}(\mathbf{k})\rho^{(1)}_{\ell m}(\mathbf{k};t) - \rho^{(1)}_{n\ell}(\mathbf{k};t) r^{\mathrm{b}}_{\ell m}(\mathbf{k}) \right)$$
$$= \sum_\ell \left(r^{\mathrm{b}}_{n\ell}(\mathbf{k}) B^{\mathrm{c}}_{\ell m}(\mathbf{k},\omega) - B^{\mathrm{c}}_{n\ell}(\mathbf{k},\omega) r^{\mathrm{b}}_{\ell m}(\mathbf{k}) \right) E^{\mathrm{c}}(t), \qquad (1.55)$$

and from Eq. (1.48)

$$R_i^{\mathrm{b}(1)}(\mathbf{k};t) = i(\rho^{(1)}_{nm}(t))_{;k^{\mathrm{b}}} = iE^{\mathrm{c}}(t)(B^{\mathrm{c}}_{nm}(\mathbf{k},\omega))_{;k^{\mathrm{b}}}. \qquad (1.56)$$

Using Eqs. (1.55) and (1.56) in Eq. (1.49), we obtain

$$\rho^{(2)}_{I,nm}(\mathbf{k};t) = \frac{ie}{\hbar}\Bigg[\sum_\ell \left(r^{\mathrm{b}}_{n\ell}(\mathbf{k}) B^{\mathrm{c}}_{\ell m}(\mathbf{k},\omega) - B^{\mathrm{c}}_{n\ell}(\mathbf{k},\omega) r^{\mathrm{b}}_{\ell m}(\mathbf{k}) \right)$$
$$+ i(B^{\mathrm{c}}_{nm}(\mathbf{k},\omega))_{;k^{\mathrm{b}}} \Bigg] E^{\mathrm{b}}_\omega E^{\mathrm{c}}_\omega \int_{-\infty}^{t} dt' e^{i(\omega^\sigma_{nm\mathbf{k}} - 2\tilde{\omega})t'}$$
$$= \frac{e}{\hbar}\Bigg[\sum_\ell \left(r^{\mathrm{b}}_{n\ell}(\mathbf{k}) B^{\mathrm{c}}_{\ell m}(\mathbf{k},\omega) - B^{\mathrm{c}}_{n\ell}(\mathbf{k},\omega) r^{\mathrm{b}}_{\ell m}(\mathbf{k}) \right)$$
$$+ i(B^{\mathrm{c}}_{nm}(\mathbf{k},\omega))_{;k^{\mathrm{b}}} \Bigg] E^{\mathrm{b}}_\omega E^{\mathrm{c}}_\omega \frac{e^{i(\omega^\sigma_{nm\mathbf{k}} - 2\tilde{\omega})t}}{\omega^\sigma_{nm\mathbf{k}} - 2\tilde{\omega}}$$
$$= e^{i\omega^\sigma_{nm\mathbf{k}} t} \rho^{(2)}_{nm}(\mathbf{k};t). \qquad (1.57)$$

Now, we write $\rho^{(2)}_{nm}(\mathbf{k};t) = \rho^{(2)}_{nm}(\mathbf{k};2\omega)e^{-i2\tilde{\omega}t}$, with

$$\rho^{(2)}_{nm}(\mathbf{k};2\omega) = \frac{e}{i\hbar}\frac{1}{\omega^\sigma_{nm\mathbf{k}} - 2\tilde{\omega}}\Bigg[- (B^{\mathrm{c}}_{nm}(\mathbf{k},\omega)_{;k^{\mathrm{b}}}$$
$$+ i\sum_\ell \left(r^{\mathrm{b}}_{n\ell} B^{\mathrm{c}}_{\ell m}(\mathbf{k},\omega) - B^{\mathrm{c}}_{n\ell}(\mathbf{k},\omega) r^{\mathrm{b}}_{\ell m} \right) \Bigg] E^{\mathrm{b}}(\omega) E^{\mathrm{c}}(\omega) \qquad (1.58)$$

where $B^{\mathrm{a}}_{\ell m}(\mathbf{k},\omega)$ are given by Eq. (1.53). We remark that $\mathbf{r}_{nm}(\mathbf{k})$ are the same whether calculated with the LDA or the scissored Hamiltonian. We chose the former in this article.

1.3 Layered Current Density

In this section, we derive the expressions for the microscopic current density of a given layer in the unit cell of the system. The approach we use to study

the surface of a semi-infinite semiconductor crystal is as follows. Instead of using a semi-infinite system, we replace it by a slab (see Fig. 1.2). The slab consists of a front and back surface, and in between these two surfaces is the bulk of the system. In general the surface of a crystal reconstructs or relaxes as the atoms move to find equilibrium positions. This is due to the fact that the otherwise balanced forces are disrupted when the surface atoms do not find their partner atoms that are now absent at the surface of the slab.

To take the reconstruction or relaxation into account, we take "surface" to mean the true surface of the first layer of atoms, and some of the atomic sub-layers adjacent to it. Since the front and the back surfaces of the slab are usually identical the total slab is centrosymmetric. This implies that $\chi^{\rm slab}_{\rm abc} = 0$, and thus we must find a way to bypass this characteristic of a centrosymmetric slab in order to have a finite $\chi^{s}_{\rm abc}$ representative of the surface. Even if the front and back surfaces of the slab are different, breaking the centrosymmetry and therefore giving an overall $\chi^{\rm slab}_{\rm abc} \neq 0$, we still need a procedure to extract the front surface $\chi^{f}_{\rm abc}$ and the back surface $\chi^{b}_{\rm abc}$ from the non-linear susceptibility $\chi^{\rm slab}_{\rm abc} = \chi^{f}_{\rm abc} - \chi^{b}_{\rm abc}$ of the entire slab.

A convenient way to accomplish the separation of the SH signal of either surface is to introduce a "cut function", $\mathcal{C}(z)$, which is usually taken to be unity over one half of the slab and zero over the other half.[11] In this case $\mathcal{C}(z)$ will give the contribution of the side of the slab for which $\mathcal{C}(z) = 1$. We can generalize this simple choice for $\mathcal{C}(z)$ by a top-hat cut function $\mathcal{C}^{\ell}(z)$ that selects a given layer,

$$\mathcal{C}^{\ell}(z) = \Theta(z - z_{\ell} + \Delta^{\rm b}_{\ell})\Theta(z_{\ell} - z + \Delta^{f}_{\ell}), \tag{1.59}$$

where Θ is the Heaviside function. Here, $\Delta^{f/b}_{\ell}$ is the distance that the ℓ-th layer extends towards the front (f) or back (b) from its z_{ℓ} position. $\Delta^{f}_{\ell} + \Delta^{b}_{\ell}$ is the thickness of layer ℓ (see Fig. 1.2).

Now, we show how this "cut function" $\mathcal{C}^{\ell}(z)$ is introduced in the calculation of $\chi_{\rm abc}$. The microscopic current density is given by

$$\mathbf{j}(\mathbf{r}, t) = {\rm Tr}(\hat{\mathbf{j}}(\mathbf{r})\hat{\rho}(t)), \tag{1.60}$$

where the operator for the electron's current is

$$\hat{\mathbf{j}}(\mathbf{r}) = \frac{e}{2}\left(\hat{\mathbf{v}}^{\sigma}|\mathbf{r}\rangle\langle\mathbf{r}| + |\mathbf{r}\rangle\langle\mathbf{r}|\hat{\mathbf{v}}^{\sigma}\right), \tag{1.61}$$

where $\hat{\mathbf{v}}^{\sigma}$ is the electron's velocity operator to be dealt with below. We

define $\hat{\mu} \equiv |\mathbf{r}\rangle\langle\mathbf{r}|$ and use the cyclic invariance of the trace to write

$$\begin{aligned}
\mathrm{Tr}(\hat{\mathbf{j}}(\mathbf{r})\hat{\rho}(t) &= \mathrm{Tr}(\hat{\rho}(t)\hat{\mathbf{j}}(\mathbf{r})) = \frac{e}{2}\left(\mathrm{Tr}(\hat{\rho}\hat{\mathbf{v}}^{\sigma}\hat{\mu}) + \mathrm{Tr}(\hat{\rho}\hat{\mu}\hat{\mathbf{v}}^{\sigma})\right) \\
&= \frac{e}{2}\sum_{n\mathbf{k}}\left(\langle n\mathbf{k}|\hat{\rho}\hat{\mathbf{v}}^{\sigma}\hat{\mu}|n\mathbf{k}\rangle + \langle n\mathbf{k}|\hat{\rho}\hat{\mu}\hat{\mathbf{v}}^{\sigma}|n\mathbf{k}\rangle\right) \\
&= \frac{e}{2}\sum_{nm\mathbf{k}}\langle n\mathbf{k}|\hat{\rho}|m\mathbf{k}\rangle\left(\langle m\mathbf{k}|\hat{\mathbf{v}}^{\sigma}|\mathbf{r}\rangle\langle\mathbf{r}|n\mathbf{k}\rangle + \langle m\mathbf{k}|\mathbf{r}\rangle\langle\mathbf{r}|\hat{\mathbf{v}}^{\sigma}|n\mathbf{k}\rangle\right) \\
\mathbf{j}(\mathbf{r},t) &= \sum_{nm\mathbf{k}}\rho_{nm}(\mathbf{k};t)\mathbf{j}_{mn}(\mathbf{k};\mathbf{r}),
\end{aligned} \tag{1.62}$$

where

$$\mathbf{j}_{mn}(\mathbf{k};\mathbf{r}) = \frac{e}{2}\left(\langle m\mathbf{k}|\hat{\mathbf{v}}^{\sigma}|\mathbf{r}\rangle\langle\mathbf{r}|n\mathbf{k}\rangle + \langle m\mathbf{k}|\mathbf{r}\rangle\langle\mathbf{r}|\hat{\mathbf{v}}^{\sigma}|n\mathbf{k}\rangle\right), \tag{1.63}$$

are the matrix elements of the microscopic current operator, and we have used the fact that the matrix elements between states $|n\mathbf{k}\rangle$ are diagonal in $\mathbf{k}$, i.e. proportional to $\delta(\mathbf{k}-\mathbf{k}')$.

Integrating the microscopic current $\mathbf{j}(\mathbf{r},t)$ over the entire slab gives the averaged microscopic current density. If we want the contribution from only one region of the unit cell towards the total current, we can integrate $\mathbf{j}(\mathbf{r},t)$ over the desired region. The contribution to the current density from the ℓ-th layer of the slab is given by

$$\frac{1}{\Omega}\int d^3r\, \mathcal{C}^{\ell}(z)\,\mathbf{j}(\mathbf{r},t) \equiv \mathbf{J}^{\ell}(t), \tag{1.64}$$

where $\mathbf{J}^{\ell}(t)$ is the microscopic current in the ℓ-th layer. Therefore we define

$$e\boldsymbol{\mathcal{V}}^{\sigma,\ell}_{mn}(\mathbf{k}) \equiv \int d^3r\, \mathcal{C}^{\ell}(z)\,\mathbf{j}_{mn}(\mathbf{k};\mathbf{r}), \tag{1.65}$$

to write

$$J^{(N,\ell)}_{a}(t) = \frac{e}{\Omega}\sum_{mn\mathbf{k}}\mathcal{V}^{\sigma,a,\ell}_{mn}(\mathbf{k})\rho^{(N)}_{nm}(\mathbf{k};t), \tag{1.66}$$

as the induced microscopic current of the ℓ-th layer, to order N in the external perturbation. The matrix elements of the density operator for $N = 1, 2$ are given by Eqs. (1.53) and (1.58) respectively. The Fourier component of microscopic current of Eq. (1.66) is given by

$$J^{(N,\ell)}_{\mathrm{a}}(\omega_3) = \frac{e}{\Omega}\sum_{mn\mathbf{k}}\mathcal{V}^{\sigma,\mathrm{a},\ell}_{mn}(\mathbf{k})\rho^{(N)}_{nm}(\mathbf{k};\omega_3). \tag{1.67}$$

We proceed to give an explicit expression of $\boldsymbol{\mathcal{V}}^{\sigma,\ell}_{mn}(\mathbf{k})$. From Eqs. (1.65) and (1.63) we obtain

$$\boldsymbol{\mathcal{V}}^{\sigma,\ell}_{mn}(\mathbf{k}) = \frac{1}{2}\int \mathrm{d}^3 r\, \mathcal{C}^\ell(z)\Big[\langle m\mathbf{k}|\mathbf{v}^\sigma|\mathbf{r}\rangle\langle\mathbf{r}|n\mathbf{k}\rangle + \langle m\mathbf{k}|\mathbf{r}\rangle\langle\mathbf{r}|\mathbf{v}^\sigma|n\mathbf{k}\rangle\Big], \quad (1.68)$$

and using the following property

$$\langle\mathbf{r}|\hat{\mathbf{v}}^\sigma(\mathbf{r},\mathbf{r}')|n\mathbf{k}\rangle = \int d^3r''\langle\mathbf{r}|\hat{\mathbf{v}}^\sigma(\mathbf{r},\mathbf{r}')|\mathbf{r}''\rangle\langle\mathbf{r}''|n\mathbf{k}\rangle = \hat{\mathbf{v}}^\sigma(\mathbf{r},\mathbf{r}'')\int d^3r''\langle\mathbf{r}|\mathbf{r}''\rangle\langle\mathbf{r}''|n\mathbf{k}\rangle = \hat{\mathbf{v}}^\sigma(\mathbf{r},\mathbf{r}')\psi_{n\mathbf{k}}(\mathbf{r}), \quad (1.69)$$

that stems from the fact that the operator $\mathbf{v}^\sigma(\mathbf{r},\mathbf{r}')$ does not act on $\mathbf{r}''$, we can write

$$\begin{aligned}\boldsymbol{\mathcal{V}}^{\sigma,\ell}_{mn}(\mathbf{k}) &= \frac{1}{2}\int \mathrm{d}^3 r\, \mathcal{C}^\ell(z)\Big[\psi_{n\mathbf{k}}(\mathbf{r})\hat{\mathbf{v}}^{\sigma *}\psi^*_{m\mathbf{k}}(\mathbf{r}) + \psi^*_{m\mathbf{k}}(\mathbf{r})\hat{\mathbf{v}}^\sigma\psi_{n\mathbf{k}}(\mathbf{r})\Big] \\ &= \int \mathrm{d}^3 r\, \psi^*_{m\mathbf{k}}(\mathbf{r})\left[\frac{\mathcal{C}^\ell(z)\mathbf{v}^\sigma + \mathbf{v}^\sigma\mathcal{C}^\ell(z)}{2}\right]\psi_{n\mathbf{k}}(\mathbf{r}) \\ &= \int \mathrm{d}^3 r\, \psi^*_{m\mathbf{k}}(\mathbf{r})\boldsymbol{\mathcal{V}}^{\sigma,\ell}\psi_{n\mathbf{k}}(\mathbf{r}). \end{aligned} \quad (1.70)$$

We used the hermitian property of $\mathbf{v}^\sigma$ and defined

$$\boldsymbol{\mathcal{V}}^{\sigma,\ell} = \frac{\mathcal{C}^\ell(z)\mathbf{v}^\sigma + \mathbf{v}^\sigma\mathcal{C}^\ell(z)}{2}, \quad (1.71)$$

where the superscript ℓ is inherited from $\mathcal{C}^\ell(z)$ and we supress the dependance on z from the increasingly crowded notation. We see that the replacement

$$\hat{\mathbf{v}}^\sigma \to \hat{\boldsymbol{\mathcal{V}}}^{\sigma,\ell} = \left[\frac{\mathcal{C}^\ell(z)\hat{\mathbf{v}}^\sigma + \hat{\mathbf{v}}^\sigma\mathcal{C}^\ell(z)}{2}\right], \quad (1.72)$$

is all that is needed to change the velocity operator of the electron $\hat{\mathbf{v}}^\sigma$ to the new velocity operator $\boldsymbol{\mathcal{V}}^{\sigma,\ell}$ that implicitly takes into account the contribution of the region of the slab given by $\mathcal{C}^\ell(z)$. From Eq. (1.25),

$$\begin{aligned}\boldsymbol{\mathcal{V}}^{\sigma,\ell} &= \boldsymbol{\mathcal{V}}^{\mathrm{LDA},\ell} + \boldsymbol{\mathcal{V}}^{\mathcal{S},\ell} \\ \boldsymbol{\mathcal{V}}^{\mathrm{LDA},\ell} &= \boldsymbol{\mathcal{V}}^{\ell} + \boldsymbol{\mathcal{V}}^{\mathrm{nl},\ell} = \frac{1}{m_e}\boldsymbol{\mathcal{P}}^\ell + \boldsymbol{\mathcal{V}}^{\mathrm{nl},\ell}. \end{aligned} \quad (1.73)$$

We remark that the simple relationship between $\mathbf{v}^\sigma_{nm}(\mathbf{k})$ and $\mathbf{v}^{\mathrm{LDA}}_{nm}(\mathbf{k})$, given in Eq. (1.29), does not hold between $\boldsymbol{\mathcal{V}}^{\sigma,\ell}_{nm}(\mathbf{k})$ and $\boldsymbol{\mathcal{V}}^{\mathrm{LDA},\ell}_{nm}(\mathbf{k})$, i.e. $\boldsymbol{\mathcal{V}}^{\sigma,\ell}_{nm}(\mathbf{k}) \neq$

$(\omega^{\sigma}_{nm}/\omega_{nm})\boldsymbol{\mathcal{V}}^{\mathrm{LDA},\ell}_{nm}(\mathbf{k})$ and $\boldsymbol{\mathcal{V}}^{\sigma,\ell}_{nn}(\mathbf{k}) \neq \boldsymbol{\mathcal{V}}^{\mathrm{LDA},\ell}_{nn}(\mathbf{k})$, and thus, to calculate $\boldsymbol{\mathcal{V}}^{\sigma,\ell}_{nm}(\mathbf{k})$ we must calculate the matrix elements of $\boldsymbol{\mathcal{V}}^{\mathcal{S},\ell}$ and $\boldsymbol{\mathcal{V}}^{\mathrm{LDA},\ell}$ (separately) according to the expressions of Appendix **??**. Aeroport Charles de Gaulle, Nov. 30, 2014, see Appendix **??**.

To limit the response to one surface, the equivalent of Eq. (1.71) for $\boldsymbol{\mathcal{V}}^{\ell} = \boldsymbol{\mathcal{P}}^{\ell}/m_e$ was proposed in Ref. [11] and later used in Refs. [12], [13], [14], and [15] also in the context of SHG. The layer-by-layer analysis of Refs. [16] and [17] used Eq. (1.59), limiting the current response to a particular layer of the slab and used to obtain the anisotropic linear optical response of semiconductor surfaces. However, the first formal derivation of this scheme is presented in Ref. [18] for the linear response, and here in this article, for the second harmonic optical response of semiconductors.

1.4 Microscopic surface susceptibility

In this section we obtain the expressions for the surface susceptibility tensor χ^{S}_{abc}. We start with the basic relation $\mathbf{J} = d\mathbf{P}/dt$ with $\mathbf{J}$ the current calculated in Sec. 1.3. From Eq. (1.67) we obtain

$$J^{(2,\ell)}_{\mathrm{a}}(2\omega) = -i2\tilde{\omega}P_{\mathrm{a}}(2\omega) = \frac{e}{\Omega}\sum_{mn\mathbf{k}}\mathcal{V}^{\sigma,\mathrm{a},\ell}_{mn}(\mathbf{k})\rho^{(2)}_{nm}(\mathbf{k};2\omega), \tag{1.74}$$

and using Eqs. (1.58) and (1.7) leads to

$$\begin{aligned}\chi^{S,\ell}_{\mathrm{abc}} &= \frac{ie}{AE^{\mathrm{b}}_1E^{\mathrm{c}}_2 2\tilde{\omega}}\sum_{mn\mathbf{k}}\mathcal{V}^{\sigma,\mathrm{a},\ell}_{mn}(\mathbf{k})\rho^{(2)}_{nm}(\mathbf{k};2\tilde{\omega}) \\ &= \frac{e^2}{A\hbar 2\tilde{\omega}}\sum_{mn\mathbf{k}}\frac{\mathcal{V}^{\sigma,\mathrm{a},\ell}_{mn}(\mathbf{k})}{\omega^{\sigma}_{nm\mathbf{k}}-2\tilde{\omega}}\Big[-\left(B^{\mathrm{c}}_{nm}(\mathbf{k},\omega)\right)_{;k^{\mathrm{b}}} \\ &\quad + i\sum_{\ell}\left(r^{\mathrm{b}}_{n\ell}B^{\mathrm{c}}_{\ell m}(\mathbf{k},\omega) - B^{\mathrm{c}}_{n\ell}(\mathbf{k},\omega)r^{\mathrm{b}}_{\ell m}\right)\Big],\end{aligned} \tag{1.75}$$

which gives the surface-like susceptibility of ℓ-th layer, where $\boldsymbol{\mathcal{V}}^{\sigma}$ is given in Eq. (1.73), where $A = \Omega/d$ is the surface area of the unit cell that characterizes the surface of the system. Using Eq. (1.53) we split this equation into two contributions from the first and second terms on the right hand side,

$$\chi^{S,\ell}_{i,\mathrm{abc}} = -\frac{e^3}{A\hbar^2 2\tilde{\omega}}\sum_{mn\mathbf{k}}\frac{\mathcal{V}^{\sigma,\mathrm{a},\ell}_{mn}}{\omega^{\sigma}_{nm}-2\tilde{\omega}}\left(\frac{f_{mn}r^{\mathrm{b}}_{nm}}{\omega^{\sigma}_{nm}-\tilde{\omega}}\right)_{;k^{\mathrm{c}}}, \tag{1.76}$$

and

$$\chi^{S,\ell}_{e,\mathrm{abc}} = \frac{ie^3}{A\hbar^2 2\tilde{\omega}} \sum_{\ell mn\mathbf{k}} \frac{\mathcal{V}^{\sigma,\mathrm{a},\ell}_{mn}}{\omega^\sigma_{nm} - 2\tilde{\omega}} \left(\frac{r^{\mathrm{c}}_{n\ell} r^{\mathrm{b}}_{\ell m} f_{m\ell}}{\omega^\sigma_{\ell m} - \tilde{\omega}} - \frac{r^{\mathrm{b}}_{n\ell} r^{\mathrm{c}}_{\ell m} f_{\ell n}}{\omega^\sigma_{n\ell} - \tilde{\omega}} \right), \tag{1.77}$$

where $\boldsymbol{\chi}^{S,\ell}_i$ is related to intraband transitions and $\boldsymbol{\chi}^{S,\ell}_e$ to interband transitions. For the generalized derivative in Eq. (1.76) we use the chain rule

$$\left(\frac{f_{mn} r^{\mathrm{b}}_{nm}}{\omega^\sigma_{nm} - \tilde{\omega}} \right)_{;k^{\mathrm{c}}} = \frac{f_{mn}}{\omega^\sigma_{nm} - \tilde{\omega}} \left(r^{\mathrm{b}}_{nm} \right)_{;k^{\mathrm{c}}} - \frac{f_{mn} r^{\mathrm{b}}_{nm} \Delta^{\mathrm{c}}_{nm}}{(\omega^\sigma_{nm} - \tilde{\omega})^2}, \tag{1.78}$$

and the following result shown in Appendix **??**,

$$(\omega^\sigma_{nm})_{;k^{\mathrm{a}}} = \left(\omega^{\mathrm{LDA}}_{nm}\right)_{;k^{\mathrm{a}}} = v^{\mathrm{LDA,a}}_{nn} - v^{\mathrm{LDA,a}}_{mm} \equiv \Delta^{\mathrm{a}}_{nm}. \tag{1.79}$$

In order to calculate the nonlinear susceptibility of any given layer ℓ we simply add the above terms $\boldsymbol{\chi}^{S,\ell} = \boldsymbol{\chi}^{S,\ell}_e + \boldsymbol{\chi}^{S,\ell}_i$ and then calculate the surface susceptibility as

$$\boldsymbol{\chi}^S \equiv \sum_{\ell=1}^{N} \boldsymbol{\chi}^{S,\ell}, \tag{1.80}$$

where $\ell = 1$ is the first layer right at the surface, and $\ell = N$ is the bulk-like layer (at a distance $\sim d$ from the surface as seen in Fig. 1.1), such that

$$\boldsymbol{\chi}^{S,\ell=N} = 0, \tag{1.81}$$

in accordance to Eq. (1.5) valid for a centrosymmetric environment. We note that the value of N is not universal. This means that the slab needs to have enough atomic layers for Eq. (1.81) to be satisfied and to give converged results for $\boldsymbol{\chi}^S$. We can use Eq. (1.80) for either the front or the back surface.

We can see from the prefactors of Eqs. (1.76) and (1.77) that they diverge as $\tilde{\omega} \to 0$. To remove this apparent divergence of $\boldsymbol{\chi}^{S,\ell}$, we perform a partial fraction expansion over $\tilde{\omega}$. As shown in Appendix **??**, we use time-reversal invariance to remove these divergences and obtain the following expressions for $\boldsymbol{\chi}^S$,

$$\mathrm{Im}[\chi^{s,\ell}_{e,\mathrm{abc},\omega}] = \frac{\pi|e|^3}{2\hbar^2} \sum_{vc\mathbf{k}} \sum_{l\neq(v,c)} \frac{1}{\omega^\sigma_{cv}} \left[\frac{\mathrm{Im}[\mathcal{V}^{\sigma,\mathrm{a},\ell}_{lc}\{r^{\mathrm{b}}_{cv} r^{\mathrm{c}}_{vl}\}]}{(2\omega^\sigma_{cv} - \omega^\sigma_{cl})} - \frac{\mathrm{Im}[\mathcal{V}^{\sigma,\mathrm{a},\ell}_{vl}\{r^{\mathrm{c}}_{lc} r^{\mathrm{b}}_{cv}\}]}{(2\omega^\sigma_{cv} - \omega^\sigma_{lv})} \right] \delta(\omega^\sigma_{cv} - \omega), \tag{1.82}$$

$$\mathrm{Im}[\chi^{s,\ell}_{i,\mathrm{abc},\omega}] = \frac{\pi|e|^3}{2\hbar^2} \sum_{cv\mathbf{k}} \frac{1}{(\omega^\sigma_{cv})^2} \left[\mathrm{Re}\left[\left\{ r^{\mathrm{b}}_{cv} \left(\mathcal{V}^{\sigma,\mathrm{a},\ell}_{vc} \right)_{;k^{\mathrm{c}}} \right\} \right] + \frac{\mathrm{Re}\left[\mathcal{V}^{\sigma,\mathrm{a},\ell}_{vc} \left\{ r^{\mathrm{b}}_{cv} \Delta^{\mathrm{c}}_{cv} \right\} \right]}{\omega^\sigma_{cv}} \right] \delta(\omega^\sigma_{cv} - \omega), \tag{1.83}$$

$$\mathrm{Im}[\chi^{s,\ell}_{e,\mathrm{abc},2\omega}] = -\frac{\pi|e|^3}{2\hbar^2}\sum_{vc\mathbf{k}}\frac{4}{\omega^\sigma_{cv}}\left[\sum_{v'\neq v}\frac{\mathrm{Im}[\mathcal{V}^{\sigma,\mathrm{a},\ell}_{vc}\{r^{\mathrm{b}}_{cv'}r^{\mathrm{c}}_{v'v}\}]}{2\omega^\sigma_{cv'}-\omega^\sigma_{cv}} - \sum_{c'\neq c}\frac{\mathrm{Im}[\mathcal{V}^{\sigma,\mathrm{a},\ell}_{vc}\{r^{\mathrm{c}}_{cc'}r^{\mathrm{b}}_{c'v}\}]}{2\omega^\sigma_{c'v}-\omega^\sigma_{cv}}\right]\delta(\omega^\sigma_{cv}-2\omega), \tag{1.84}$$

and

$$\mathrm{Im}[\chi^{s,\ell}_{i,\mathrm{abc},2\omega}] = \frac{\pi|e|^3}{2\hbar^2}\sum_{vc\mathbf{k}}\frac{4}{(\omega^\sigma_{cv})^2}\left[\mathrm{Re}\left[\mathcal{V}^{\sigma,\mathrm{a},\ell}_{vc}\left\{\left(r^{\mathrm{b}}_{cv}\right)_{;k^{\mathrm{c}}}\right\}\right] - \frac{2\mathrm{Re}\left[\mathcal{V}^{\sigma,\mathrm{a},\ell}_{vc}\left\{r^{\mathrm{b}}_{cv}\Delta^{\mathrm{c}}_{cv}\right\}\right]}{\omega^\sigma_{cv}}\right]\delta(\omega^\sigma_{cv}-2\omega), \tag{1.85}$$

where the limit of $\eta \to 0$ has been taken. We have split the interband and intraband 1ω and 2ω contributions. The real part of each contribution can be obtained through a Kramers-Kronig transformation,[19] and then $\chi^{S,\ell}_{\mathrm{abc}} = \chi^{S,\ell}_{e,\mathrm{abc},\omega}+\chi^{S,\ell}_{e,\mathrm{abc},2\omega}+\chi^{S,\ell}_{i,\mathrm{abc},\omega}+\chi^{S,\ell}_{i,\mathrm{abc},2\omega}$. To fulfill the required intrinsic permutation symmetry,[20] the $\{\}$ notation symmetrizes the bc Cartesian indices, i.e. $\{u^{\mathrm{b}}s^{\mathrm{c}}\} = (u^{\mathrm{b}}s^{\mathrm{c}}+u^{\mathrm{c}}s^{\mathrm{b}})/2$, and thus $\chi^{S,\ell}_{\mathrm{abc}} = \chi^{S,\ell}_{\mathrm{acb}}$. In Appendices **??** and **??** we demonstrate how to calculate the generalized derivatives of $\mathbf{r}_{nm;\mathbf{k}}$ and $\mathcal{V}^{\sigma,\mathrm{a},\ell}_{nm;\mathbf{k}}$. We find that

$$(r^{\mathrm{b}}_{nm})_{;k^{\mathrm{a}}} = -i\mathcal{T}^{\mathrm{ab}}_{nm} + \frac{r^{\mathrm{a}}_{nm}\Delta^{\mathrm{b}}_{mn}+r^{\mathrm{b}}_{nm}\Delta^{\mathrm{a}}_{mn}}{\omega^{\mathrm{LDA}}_{nm}} + \frac{i}{\omega^{\mathrm{LDA}}_{nm}}\sum_{\ell}\left(\omega^{\mathrm{LDA}}_{\ell m}r^{\mathrm{a}}_{n\ell}r^{\mathrm{b}}_{\ell m} - \omega^{\mathrm{LDA}}_{n\ell}r^{\mathrm{b}}_{n\ell}r^{\mathrm{a}}_{\ell m}\right), \tag{1.86}$$

where

$$\mathcal{T}^{\mathrm{ab}}_{nm} = [r^{\mathrm{a}}, v^{\mathrm{LDA,b}}] = \frac{i\hbar}{m_e}\delta_{ab}\delta_{nm} + \mathcal{L}^{\mathrm{ab}}_{nm}, \tag{1.87}$$

and

$$\mathcal{L}^{\mathrm{ab}}_{nm} = \frac{1}{i\hbar}[r^{\mathrm{a}}, v^{\mathrm{nl,b}}]_{nm}, \tag{1.88}$$

is the contribution to the generalized derivative of $\mathbf{r}_{nm}$ coming from the nonlocal part of the pseudopotential. In Appendix **??** we calculate $\mathcal{L}^{\mathrm{ab}}_{nm}$, that is a term with very small numerical value but with a computational time at least an order of magnitude larger than for all the other terms involved in the expressions for $\chi^{s,\ell}_{\mathrm{abc}}$.[21] Therefore, we neglect it throughout this article and take

$$\mathcal{T}^{\mathrm{ab}}_{nm} \approx \frac{i\hbar}{m_e}\delta_{ab}\delta_{nm}. \tag{1.89}$$

Finally, we also need the following term (Eq. (**??**))

$$(v_{nn}^{\mathrm{LDA,a}})_{;k^{\mathrm{b}}} = \nabla_{k^{\mathrm{a}}} v_{nn}^{\mathrm{LDA,b}}(\mathbf{k}) = -i\mathcal{T}_{nn}^{\mathrm{ab}} - \sum_{\ell\neq n} \omega_{\ell n}^{\mathrm{LDA}} \left(r_{n\ell}^{\mathrm{a}} r_{\ell n}^{\mathrm{b}} + r_{n\ell}^{\mathrm{b}} r_{\ell n}^{\mathrm{a}} \right)$$
$$\approx \frac{\hbar}{m_e}\delta_{\mathrm{ab}} - \sum_{\ell\neq n} \omega_{\ell n}^{\mathrm{LDA}} \left(r_{n\ell}^{\mathrm{a}} r_{\ell n}^{\mathrm{b}} + r_{n\ell}^{\mathrm{b}} r_{\ell n}^{\mathrm{a}} \right), \tag{1.90}$$

among other quantities for $\mathcal{V}_{nm;\mathbf{k}}^{\sigma,\mathrm{a},\ell}$, where we also use Eq. (1.89). Above is the standard effective-mas sum rule. [22]

1.5 Conclusions

We have presented a complete derivation of the required elements to calculate in the independent particle approach (IPA) the microscopic surface second harmonic susceptibility tensor $\boldsymbol{\chi}^S(-2\omega;\omega,\omega)$ using a layer-by-layer approach. We have done so for semiconductors using the length gauge for the coupling of the external electric field to the electron.

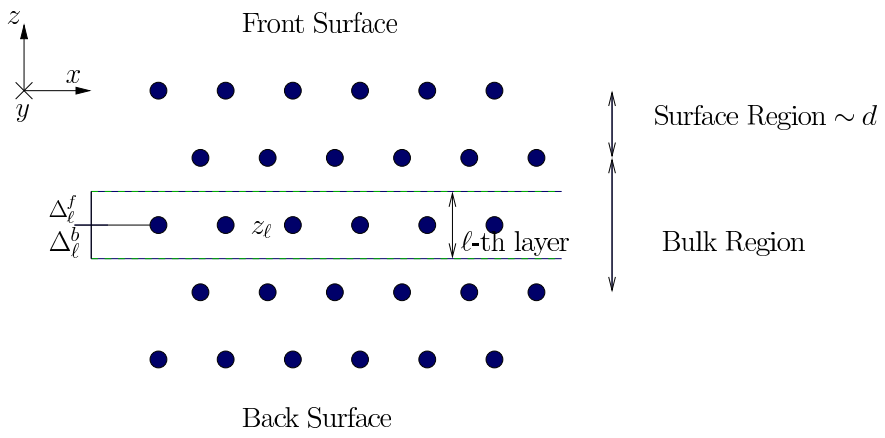

Figure 1.2: A sketch of a slab where the circles represent atoms.

Chapter 2

SHG Yield

2.1 Three layer model for SHG radiation

In this section we derive the formulas required for the calculation of the SHG yield, defined by

$$\mathcal{R}(\omega) = \frac{I(2\omega)}{I^2(\omega)}, \tag{2.1}$$

with the intensity in the MKS system is given by[23]

$$I(\omega) = 2n(\omega)\epsilon_0 c|E(\omega)|^2, \tag{2.2}$$

where $n(\omega) = \sqrt{\epsilon(\omega)}$ is the index of refraction with $\epsilon(\omega)$ the dielectric function, ϵ_0 is the vacuum permittivity, and c the speed of light in vacuum.

There are several ways to calculate R, one of which is the procedure followed by Cini [24]. This approach calculates the nonlinear susceptibility and at the same time the radiated fields. However, we present an alternative derivation based in the work of Mizrahi and Sipe [25], since the derivation of the three-layer-model is straightforward. In this scheme, we represent the surface by three regions or layers. The first layer is the vacuum region (denoted by v) with a dielectric function $\epsilon_v(\omega) = 1$ from where the fundamental electric field $\mathbf{E}_v(\omega)$ impinges on the material. The second layer is a thin layer (denoted by ℓ) of thickness d characterized by a dielectric function $\epsilon_\ell(\omega)$. Is in this layer where the second harmonic generation takes place. The third layer is the bulk region denoted by b and characterized by $\epsilon_b(\omega)$. Both the vacuum layer and the bulk layer are semiinfinite (see Fig. 2.1).

To model the electromagnetic response of the three-layer model we follow Ref. [25], and assume a polarization sheet of the form

$$\mathbf{P}(\mathbf{r}, t) = \boldsymbol{\mathcal{P}} e^{i\boldsymbol{\kappa}\cdot\mathbf{R}} e^{-i\omega t}\delta(z - z_\beta) + \text{c.c.}, \tag{2.3}$$

where $\mathbf{R} = (x, y)$, $\boldsymbol{\kappa}$ is the component of the wave vector $\boldsymbol{\nu}_\beta$ paralel to the surface, and z_β is the position of the sheet within medium β (see Fig. 2.1).

In Ref. [26] it has been shown that the solution of the Maxwell equations for the radiated fields $E_{\beta,p\pm}$ and $E_{\beta,s}$ with $\mathbf{P}(\mathbf{r},t)$as a source can be written, at points $z \neq 0$, as

$$(E_{\beta,p\pm}, E_{\beta,s}) = (\frac{\gamma i\tilde{\omega}^2}{\tilde{w}_\beta}\,\hat{\mathbf{p}}_{\beta\pm}\cdot\boldsymbol{\mathcal{P}}, \frac{\gamma i\tilde{\omega}^2}{\tilde{w}_\beta}\,\hat{\mathbf{s}}\cdot\boldsymbol{\mathcal{P}}), \tag{2.4}$$

where $\gamma = 2\pi$ in cgs units and $\gamma = 1/2\epsilon_0$ in MKS units. Also, $\hat{\mathbf{s}}$ and $\hat{\mathbf{p}}_{\beta\pm}$ are the unitary vectors for the s and p polarization of the radiated field, respectively, and the $\pm$ refers to upward $(+)$ or downward $(-)$ direction of propagation within medium β, as shown in Fig. 2.1, and $\tilde{\omega} = \omega/c$. Also, $\tilde{w}_\beta(\omega) = \tilde{\omega} w_\beta$, where

$$w_\beta(\omega) = \left(\epsilon_\beta(\omega) - \sin^2\theta_0\right)^{1/2}, \tag{2.5}$$

where θ_0 is the angle of incidence of $\mathbf{E}_v(\omega)$, and

$$\hat{\mathbf{p}}_{\beta\pm}(\omega) = \frac{\kappa(\omega)\hat{\mathbf{z}} \mp \tilde{w}_\beta(\omega)\hat{\boldsymbol{\kappa}}}{\tilde{\omega} n_\beta(\omega)} = \frac{\sin\theta_0\hat{\mathbf{z}} \mp w_\beta(\omega)\hat{\boldsymbol{\kappa}}}{n_\beta(\omega)}, \tag{2.6}$$

where $\kappa(\omega) = |\boldsymbol{\kappa}| = \tilde{\omega}\sin\theta_0$, $n_\beta(\omega) = \sqrt{\epsilon_\beta(\omega)}$ is the index of refraction of medium β, and z is the direction perpendicular to the surface that points towards the vacuum. We chose the plane of incidence along the $\boldsymbol{\kappa}z$ plane, then

$$\hat{\boldsymbol{\kappa}} = \cos\phi\hat{\mathbf{x}} + \sin\phi\hat{\mathbf{y}}, \tag{2.7}$$

and

$$\hat{\mathbf{s}} = -\sin\phi\hat{\mathbf{x}} + \cos\phi\hat{\mathbf{y}}, \tag{2.8}$$

where ϕ the angle with respect to the x axis.

In the three-layer model the nonlinear polarization responsible for the second harmonic generation (SHG) is immersed in the thin $\beta = \ell$ layer, and is given by

$$\mathcal{P}_i(2\omega) = \begin{cases} \chi_{ijk}(2\omega)E_j(\omega)E_k(\omega) & \text{(cgs units)} \\ \epsilon_0\chi_{ijk}(2\omega)E_j(\omega)E_k(\omega) & \text{(MKS units)} \end{cases}, \tag{2.9}$$

where the tensor $\boldsymbol{\chi}(2\omega)$ is the surface nonlinear dipolar susceptibility and the Cartesian indices i, j, k are summed if repeated. Also, $\chi_{ijk}(2\omega) = \chi_{ikj}(2\omega)$ is the intrinsic permutation symmetry due to the fact that SHG is degenerate in $E_j(\omega)$ and $E_k(\omega)$. As it was done in Ref. [25], in presenting the results Eq. (2.4)-(2.8) we have taken the polarization sheet (Eq. (2.3))

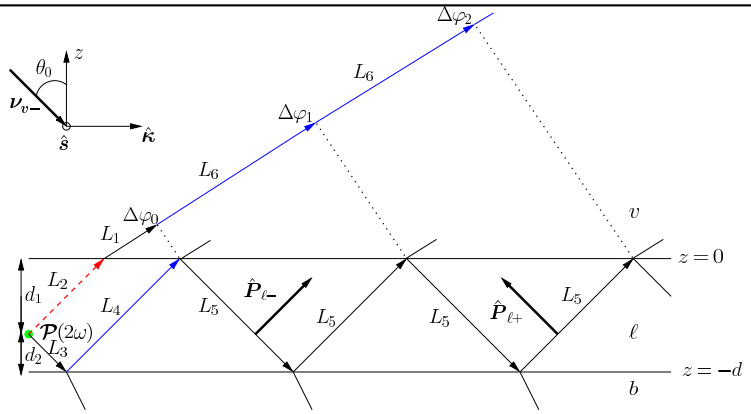

Figure 2.1: Sketch of the three layer model for SHG. Vacuum (v) is on top with $\epsilon_v = 1$; the layer ℓ, of thickness $d = d_1 + d_2$, is characterized with $\epsilon_\ell(\omega)$, and it is where the SH polarization sheet $\boldsymbol{\mathcal{P}}(2\omega)$ is located at $z_\ell = d_1$; The bulk b is described with $\epsilon_b(\omega)$. The arrows point along the direction of propagation, and the p-polarization unit vector, $\hat{\mathbf{P}}_{\ell-(+)}$, along the downward (upward) direction is denoted with a thick arrow. The s-polarization unit vector $\hat{\mathbf{s}}$, points out of the page. The fundamental field $\mathbf{E}(\omega)$ is incident from the vacuum side along the $z\hat{\boldsymbol{\kappa}}$-plane, with θ_0 its angle of incidence and $\boldsymbol{\nu}_{v-}$ its wave vector. $\Delta\varphi_i$ denote the phase difference of the multiply reflected beams with respect to the first vacuum transmitted beam (dashed-red arrow), where the dotted lines are perpendicular to this beam (see the text for details).

to be oscillating at some frequency ω. However, in the following we find it convenient to use ω exclusively to denote the fundamental frequency and $\boldsymbol{\kappa}$ to denote the component of the incident wave vector parallel to the surface. Then the nonlinear generated polarization is oscillating at $\Omega = 2\omega$ and will be characterized by a wave vector parallel to the surface $\mathbf{K} = 2\boldsymbol{\kappa}$. We can carry over Eqs. (2.3)-(2.8) simply by replacing the lowercase symbols $(\omega, \tilde{\omega}, \boldsymbol{\kappa}, n_\beta, \tilde{w}_\beta, w_\beta, \hat{\mathbf{p}}_{\beta\pm}, \hat{\mathbf{s}})$ with uppercase symbols $(\Omega, \tilde{\Omega}, \mathbf{K}, N_\beta, \tilde{W}_\beta, W_\beta, \hat{\mathbf{P}}_{\beta\pm}, \hat{\mathbf{S}})$, all evaluated at 2ω and we always have $\hat{\mathbf{S}} = \hat{\mathbf{s}}$.

To describe the propagation of the SH field, we see from Fig. 2.1, that it is refracted at the layer-vacuum interface (ℓv), and multiply reflected from the layer-bulk (ℓb) and layer-vacuum (ℓv) interfaces, thus we can define,

$$\mathbf{T}^{\ell v} = \hat{\mathbf{s}} T_s^{\ell v} \hat{\mathbf{s}} + \hat{\mathbf{P}}_{v+} T_p^{\ell v} \hat{\mathbf{P}}_{\ell+}, \tag{2.10}$$

as the tensor for transmission from ℓv interface,

$$\mathbf{R}^{\ell b} = \hat{\mathbf{s}} R_s^{\ell b} \hat{\mathbf{s}} + \hat{\mathbf{P}}_{\ell +} R_p^{\ell b} \hat{\mathbf{P}}_{\ell -}, \tag{2.11}$$

as the tensor of reflection from the ℓb interface, and

$$\mathbf{R}^{\ell v} = \hat{\mathbf{s}} R_s^{\ell v} \hat{\mathbf{s}} + \hat{\mathbf{P}}_{\ell -} R_p^{\ell v} \hat{\mathbf{P}}_{\ell +}, \tag{2.12}$$

as that of the ℓv interface. The Fresnel factors in uppercase letters, $T_{s,p}^{ij}$ and $R_{s,p}^{ij}$, are evaluated at 2ω from the following well known formulas

$$\begin{aligned} t_s^{ij}(\omega) &= \frac{2k_i(\omega)}{k_i(\omega)+k_j(\omega)}, \qquad & t_p^{ij}(\omega) &= \frac{2k_i(\omega)\sqrt{\epsilon_i(\omega)\epsilon_j(\omega)}}{k_i(\omega)\epsilon_j(\omega)+k_j(\omega)\epsilon_i(\omega)}, \\ r_s^{ij}(\omega) &= \frac{k_i(\omega)-k_j(\omega)}{k_i(\omega)+k_j(\omega)}, \qquad & r_p^{ij}(\omega) &= \frac{k_i(\omega)\epsilon_j(\omega)-k_j\epsilon_i(\omega)}{k_i(\omega)\epsilon_j(\omega)+k_j(\omega)\epsilon_i(\omega)}. \end{aligned} \tag{2.13}$$

From these expressions one can show that,

$$\begin{aligned} 1 + r_s^{\ell b} &= t_s^{\ell b} \\ 1 + r_p^{\ell b} &= \frac{n_b}{n_\ell} t_p^{\ell b} \\ 1 - r_p^{\ell b} &= \frac{n_\ell}{n_b}\frac{w_b}{w_\ell} t_p^{\ell b} \\ t_p^{\ell v} &= \frac{w_\ell}{w_v} t_p^{v\ell} \\ t_s^{\ell v} &= \frac{w_\ell}{w_v} t_s^{v\ell}. \end{aligned} \tag{2.14}$$

2.1.1 Multiple SH reflections

The SH field $\mathbf{E}(2\omega)$ radiated by the SH polarization $\boldsymbol{\mathcal{P}}(2\omega)$ will radiate directly into vacuum and also into the bulk, where it will be reflected back at the thin-layer-bulk interface into the thin layer again and this beam will be multiple-transmitted and reflected as shown in Fig. 2.1. As the two beams propagate a phase difference will develop between them, according to

$$\begin{aligned} \Delta\varphi_m &= \tilde{\Omega}\Big((L_3 + L_4 + 2mL_5)N_\ell - \big(L_2 N_\ell + (L_1 + mL_6)N_v\big)\Big) \\ &= \delta_0 + m\delta \quad m = 0, 1, 2, \ldots, \end{aligned} \tag{2.15}$$

where

$$\delta_0 = 8\pi \left(\frac{d_2}{\lambda_0}\right) \sqrt{n_\ell^2(2\omega) - \sin^2\theta_0}, \tag{2.16}$$

$$\delta = 8\pi \left(\frac{d}{\lambda_0}\right) \sqrt{n_\ell^2(2\omega) - \sin^2\theta_0}, \tag{2.17}$$

where λ_0 is the wavelength of the fundamental field in vacuum, d the thickness of layer ℓ and d_2 the distance of $\boldsymbol{\mathcal{P}}(2\omega)$ from the ℓb interface (see Fig. 2.1). We see that δ_0 is the phase difference of the first and second transmitted beams, and $m\delta$ that of the first and third ($m = 1$), fourth ($m = 2$), etc. beams (see Fig. 2.1).

To take into account the multiple reflections of the generated SH field in the layer ℓ, we proceed as follows. We show the algebra for the p-polarized SH field, the s-polarized field could be worked out along the same steps. The multiple-reflected $\mathbf{E}_p(2\omega)$ field is given by

$$\begin{aligned}\mathbf{E}(2\omega) &= E_{p+}(2\omega)\mathbf{T}^{\ell v}\cdot\hat{\mathbf{P}}_{\ell+} + E_{p-}(2\omega)\mathbf{T}^{\ell v}\cdot\mathbf{R}^{\ell b}\cdot\hat{\mathbf{P}}_{\ell-}e^{i\Delta\varphi_0} + E_{p-}(2\omega)\mathbf{T}^{\ell v}\cdot\mathbf{R}^{\ell b}\cdot\mathbf{R}^{\ell v}\cdot\mathbf{R}^{\ell b}\cdot\hat{\mathbf{P}}_{\ell-}e^{i\Delta\varphi_1}\\ &\quad + E_{p-}(2\omega)\mathbf{T}^{\ell v}\cdot\mathbf{R}^{\ell b}\cdot\mathbf{R}^{\ell v}\cdot\mathbf{R}^{\ell b}\cdot\mathbf{R}^{\ell v}\cdot\mathbf{R}^{\ell b}\cdot\hat{\mathbf{P}}_{\ell-}e^{i\Delta\varphi_2}+\cdots\\ &= E_{p+}(2\omega)\mathbf{T}^{\ell v}\cdot\hat{\mathbf{P}}_{\ell+} + E_{p-}(2\omega)\mathbf{T}^{\ell v}\cdot\sum_{m=0}^{\infty}\left(\mathbf{R}^{\ell b}\cdot\mathbf{R}^{\ell v}e^{i\delta}\right)^m\cdot\mathbf{R}^{\ell b}\cdot\hat{\mathbf{P}}_{\ell-}e^{i\delta_0}.\end{aligned} \tag{2.18}$$

From Eqs. (2.10)-(2.12) is easy to show that

$$\mathbf{T}^{\ell v}\cdot\left(\mathbf{R}^{\ell b}\cdot\mathbf{R}^{\ell v}\right)^n\cdot\mathbf{R}^{\ell b} = \hat{\mathbf{s}}T_s^{\ell v}\left(R_s^{\ell b}R_s^{\ell v}\right)^n R_s^{\ell b}\hat{\mathbf{s}} + \hat{\mathbf{P}}_{v+}T_p^{\ell v}\left(R_p^{\ell b}R_p^{\ell v}\right)^n R_p^{\ell b}\hat{\mathbf{P}}_{\ell-}, \tag{2.19}$$

then,

$$\mathbf{E}(2\omega) = \hat{\mathbf{P}}_{\ell+}T_p^{\ell v}\left(E_{p+}(2\omega) + \frac{R_p^{\ell b}e^{i\delta_0}}{1+R_p^{v\ell}R_p^{\ell b}e^{i\delta}}E_{p-}(2\omega)\right), \tag{2.20}$$

where we used $R_{s,p}^{ij} = -R_{s,p}^{ji}$. Using Eq. (2.4), we can readily write

$$\mathbf{E}(2\omega) = \frac{\gamma i\tilde{\Omega}}{W_\ell}\mathbf{H}_\ell\cdot\boldsymbol{\mathcal{P}}(2\omega), \tag{2.21}$$

where

$$\mathbf{H}_\ell = \hat{\mathbf{s}}\,T_s^{\ell v}\left(1+R_s^M\right)\hat{\mathbf{s}} + \hat{\mathbf{P}}_{v+}T_p^{\ell v}\left(\hat{\mathbf{P}}_{\ell+} + R_p^M\hat{\mathbf{P}}_{\ell-}\right). \tag{2.22}$$

and

$$R_l^M \equiv \frac{R_l^{\ell b}e^{i\delta_0}}{1+R_l^{v\ell}R_l^{\ell b}e^{i\delta}} \quad l = s,p, \tag{2.23}$$

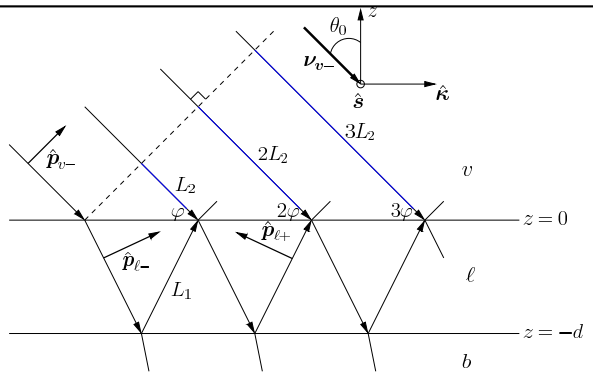

Figure 2.2: (color on line) Sketch for the multiple reflected fundamental field $\mathbf{E}(\omega)$, which impinges from the vacuum side along the $z\hat{\boldsymbol{\kappa}}$-plane, with θ_0 and $\boldsymbol{\nu}_{v-}$ its angle of incidence and wave vector, respectively. The arrows point along the direction of propagation. The p-polarization unit vectors, $\hat{\mathbf{p}}_{\beta\pm}$, along the downward (-) or upward (+) direction are denoted with thick arrows, where $\beta = v$ or ℓ. The s-polarization unit vector $\hat{\mathbf{s}}$ points out of the page, and $(1, 2, 3, \ldots)\phi$ denotes the phase difference for the multiply reflected beams with respect to the incident field, where the dotted line is perpendicular to this beam (see the text for details).

is defined as the multiple (M) reflection coefficient. To make touch with the work of Ref. [25] where $\boldsymbol{\mathcal{P}}(2\omega)$ is located on top of the vacuum-surface interface and only the vacuum radiated beam and the first (and only) reflected beam need to be considered, we take $\ell = v$ and $d_2 = 0$, then $T^{\ell v} = 1$, $R^{v\ell} = 0$ and $\delta_0 = 0$, with which $R_l^M = R_l^{vb}$. Thus, Eq. (2.22) coincides with Eq. (3.8) of Ref. [25].

2.1.2 Multiple reflections for the linear field

Similar to the SH field, here we consider the multiple reflections of the fundamental field $\mathbf{E}(\omega)$ inside the thin ℓ layer. In Fig. 2.2 we show the situation where $\mathbf{E}(\omega)$ impinges from the vacuum side with an angle of incidence θ_0. As the first transmitted beam is multiply reflected from the ℓb and the ℓv interfaces, it accumulates a phase difference of $n\phi$, with $n = 1, 2, 3, \ldots$, given

by

$$\begin{aligned}\phi &= \frac{\omega}{c}(2L_1 n_\ell - L_2 n_v) \\ &= 4\pi\left(\frac{d}{\lambda_0}\right)\sqrt{n_\ell^2 - \sin^2\theta_0},\end{aligned} \tag{2.24}$$

where $n_v = 1$. Besides the equivalent of Eqs. (2.11) and (2.12), for ω, we also need

$$\mathbf{t}^{v\ell} = \hat{\mathbf{s}} t_s^{v\ell} \hat{\mathbf{s}} + \hat{\mathbf{p}}_{\ell-} t_p^{v\ell} \hat{\mathbf{p}}_{v-}, \tag{2.25}$$

to write

$$\begin{aligned}\mathbf{E}(\omega) &= E_0\left[\mathbf{t}^{v\ell} + \mathbf{r}^{\ell b}\cdot\mathbf{t}^{v\ell}e^{i\phi} + \mathbf{r}^{\ell b}\cdot\mathbf{r}^{\ell v}\cdot\mathbf{r}^{\ell b}\cdot\mathbf{t}^{v\ell}e^{i2\phi} + \mathbf{r}^{\ell b}\cdot\mathbf{r}^{\ell v}\cdot\mathbf{r}^{\ell b}\cdot\mathbf{r}^{\ell v}\cdot\mathbf{r}^{\ell b}\cdot\mathbf{t}^{v\ell}e^{i3\phi} + \cdots\right]\cdot\mathbf{e}^{\text{in}} \\ &= E_0\left[1 + \left(1 + \mathbf{r}^{\ell b}\cdot\mathbf{r}^{\ell v}e^{i\phi} + (\mathbf{r}^{\ell b}\cdot\mathbf{r}^{\ell v})^2 e^{i2\phi} + \cdots\right)\cdot\mathbf{r}^{\ell b}e^{i\phi}\right]\cdot\mathbf{t}^{v\ell}\cdot\mathbf{e}^{\text{in}} \\ &= E_0\left[\hat{\mathbf{s}} t_s^{v\ell}(1 + r_s^M)\hat{\mathbf{s}} + t_p^{v\ell}\left(\hat{\mathbf{p}}_{\ell-} + \hat{\mathbf{p}}_{\ell+} r_p^M\right)\hat{\mathbf{p}}_{v-}\right]\cdot\mathbf{e}^{\text{in}}\end{aligned} \tag{2.26}$$

where

$$r_l^M = \frac{r_l^{\ell b} e^{i\phi}}{1 + r_l^{v\ell} r_l^{\ell b} e^{i\phi}} \quad l = s, p. \tag{2.27}$$

We define $\mathbf{E}^l(\omega) \equiv E_0 \mathbf{e}_\ell^{\omega,l}$ $(l = s, p)$, where using Eq. (2.6), we obtain that

$$\mathbf{e}_\ell^{\omega,p} = \frac{t_p^{v\ell}}{n_\ell}\left(r_p^{M+}\sin\theta_0\hat{\mathbf{z}} + r_p^{M-} w_\ell \hat{\boldsymbol{\kappa}}\right), \tag{2.28}$$

for p-input polarization, i.e. $\mathbf{e}^{\text{in}} = \hat{\mathbf{p}}_{v-}$, and

$$\mathbf{e}_\ell^{\omega,s} = t_s^{v\ell} r_s^{M+}\hat{\mathbf{s}}, \tag{2.29}$$

for s-input polarization, i.e. $\mathbf{e}^{\text{in}} = \hat{\mathbf{s}}$, where

$$r_l^{M\pm} = 1 \pm r^M \quad l = s, p. \tag{2.30}$$

2.1.3 SHG Yield

The magnitude of the radiated field is given by $E(2\omega) = \hat{\mathbf{e}}^{\text{out}}\cdot\mathbf{E}(2\omega)$, where $\hat{\mathbf{e}}^{\text{out}}$ is the polarization vector of the radiated field, for instance $\hat{\mathbf{s}}$ or $\hat{\mathbf{P}}_{v+}$. Then, we write

$$\begin{aligned}\hat{\mathbf{P}}_{\ell+} + R_p^M\hat{\mathbf{P}}_{\ell-} &= \frac{\sin\theta_0\hat{\mathbf{z}} - W_\ell\hat{\boldsymbol{\kappa}}}{N_\ell} + R_p^M\frac{\sin\theta_0\hat{\mathbf{z}} + W_\ell\hat{\boldsymbol{\kappa}}}{N_\ell} \\ &= \frac{1}{N_\ell}\left(\sin\theta_0 R_{p+}^M\hat{\mathbf{z}} - K_\ell R_{p-}^M\hat{\boldsymbol{\kappa}}\right),\end{aligned} \tag{2.31}$$

where

$$R_l^{M\pm} \equiv 1 \pm R_l^M \quad l = s, p. \tag{2.32}$$

Using Eq. (2.14) we write Eq. (2.21) as

$$E(2\omega) = \frac{2\gamma i\omega}{cW_\ell}\hat{\mathbf{e}}^{\text{out}} \cdot \mathbf{H}_\ell \cdot \boldsymbol{\mathcal{P}}(2\omega) = \frac{2\gamma i\omega}{cW_v}\mathbf{e}_\ell^{2\omega} \cdot \boldsymbol{\mathcal{P}}(2\omega). \tag{2.33}$$

$$\mathbf{e}_\ell^{2\omega} = \hat{\mathbf{e}}^{\text{out}} \cdot \left[\hat{\mathbf{s}}T_s^{v\ell}R_s^{M+}\hat{\mathbf{s}} + \hat{\mathbf{P}}_{v+}\frac{T_p^{v\ell}}{N_\ell}\left(\sin\theta_0 R_p^{M+}\hat{\mathbf{z}} - W_\ell R_p^{M-}\hat{\boldsymbol{\kappa}}\right)\right]. \tag{2.34}$$

We pause here to reduce above result to the case where the nonlinear polarization $\mathbf{P}(2\omega)$ radiates from vacuum instead from the layer ℓ. For such case we simply take $\epsilon_\ell(2\omega) = 1$ and $\ell = v$ ($T_{s,p}^{\ell v} = 1$), to get

$$\mathbf{e}_v^{2\omega} = \hat{\mathbf{e}}^{\text{out}} \cdot \left[\hat{\mathbf{s}}T_s^{vb}\hat{\mathbf{s}} + \hat{\mathbf{P}}_{v+}\frac{T_p^{vb}}{\sqrt{\epsilon_b(2\omega)}}\left(\epsilon_b(2\omega)\sin\theta_0\hat{\mathbf{z}} - W_b\hat{\boldsymbol{\kappa}}\right)\right], \tag{2.35}$$

which agrees with Eq. (3.10) of Ref. [25].

In the three layer model the SH polarization $\boldsymbol{\mathcal{P}}(2\omega)$ is located in layer ℓ, where we evaluate the fundamental field required in Eq. (2.9). We write

$$\mathbf{E}_\ell(\omega) = E_0\left(\hat{\mathbf{s}}t_s^{v\ell}(1 + r_s^{\ell b})\hat{\mathbf{s}} + \hat{\mathbf{p}}_{\ell-}t_p^{v\ell}\hat{\mathbf{p}}_{v-} + \hat{\mathbf{p}}_{\ell+}t_p^{v\ell}r_p^{\ell b}\hat{\mathbf{p}}_{v-}\right) \cdot \hat{\mathbf{e}}^{\text{in}} = E_0\mathbf{e}_\ell^\omega, \tag{2.36}$$

where $\mathbf{e}^{\text{in}}$ is the s ($\hat{\mathbf{s}}$) or p ($\hat{\mathbf{p}}_{v-}$) incoming polarization of the fundamental electric field. Above field is composed of the transmitted field and its first reflection from the ℓb interface for s and p polarizations. The fundamental field, once inside the layer ℓ will be multiply reflected at the ℓv and ℓb interfaces, however each reflection will diminish the intensity of the fundamental field, and as the SHG yield goes with the square of this field, the contribution of the subsequent reflections, other than the one considered in Eq. (2.36), could be safely neglected. From Eq. (2.14) we find that

$$\mathbf{e}_\ell^\omega = \left[\hat{\mathbf{s}}t_s^{v\ell}t_s^{\ell b}\hat{\mathbf{s}} + \frac{t_p^{v\ell}t_p^{\ell b}}{n_\ell^2 n_b}\left(n_b^2\sin\theta_0\hat{\mathbf{z}} + n_\ell^2 w_b\hat{\boldsymbol{\kappa}}\right)\hat{\mathbf{p}}_{v-}\right] \cdot \hat{\mathbf{e}}^{\text{in}}. \tag{2.37}$$

Again, to touch base with Ref. [25], if we would like to evaluate the fields in the bulk, instead of the layer ℓ, we simply take $n_\ell = n_b$, ($t_{s,p}^{\ell b} = 1$), to obtain

$$\mathbf{e}_b^\omega = \left[\hat{\mathbf{s}}t_s^{vb}\hat{\mathbf{s}} + \frac{t_p^{vb}}{n_b}\left(\sin\theta_0\hat{\mathbf{z}} + w_b\hat{\boldsymbol{\kappa}}\right)\hat{\mathbf{p}}_{v-}\right] \cdot \hat{\mathbf{e}}^{\text{in}}, \tag{2.38}$$

that is in agreement with Eq. (3.5) of Ref. [25]. Then, we can write Eq. (2.9) as

$$\boldsymbol{\mathcal{P}}(2\omega) = \begin{cases} E_0^2\, \boldsymbol{\chi} : \mathbf{e}_\ell^\omega \mathbf{e}_\ell^\omega & \text{(cgs units)} \\ \epsilon_0 E_0^2\, \boldsymbol{\chi} : \mathbf{e}_\ell^\omega \mathbf{e}_\ell^\omega & \text{(MKS units)} \end{cases}, \tag{2.39}$$

where E_0 is the intensity of the fundamental electric field. Finally, with above equation we write Eq. (2.33) as

$$E(2\omega) = \frac{2\eta i\omega}{cW_v} \mathbf{e}_\ell^{2\omega} \cdot \boldsymbol{\chi} : \mathbf{e}_\ell^\omega \mathbf{e}_\ell^\omega, \tag{2.40}$$

where $\eta = 2\pi$ for cgs units and $\eta = 1/2$ for MKS units. To ease on the notation, we define

$$\Upsilon_{\mathrm{iO}} \equiv \mathbf{e}_\ell^{2\omega} \cdot \boldsymbol{\chi} : \mathbf{e}_\ell^\omega \mathbf{e}_\ell^\omega, \tag{2.41}$$

where i stands for the incoming polarization of the fundamental electric field given by $\hat{\mathbf{e}}^{\mathrm{in}}$ in Eq. (2.37), and O for the outgoing polarization of the SH electric field given by $\hat{\mathbf{e}}^{\mathrm{out}}$ in Eq. (2.34).

From Eqs. (2.1) and (2.2) we obtain that in the cgs units ($\eta = 2\pi$)

$$\begin{aligned} |E(2\omega)|^2 &= |E_0|^4 \frac{16\pi^2\omega^2}{c^2 W_v^2} |\Upsilon_{\mathrm{iO}}|^2 \\ \frac{c}{2\pi}|\sqrt{N_v}E(2\omega)|^2 &= \frac{32\pi^3\omega^2}{c^3\cos^2\theta_0} \left|\frac{\sqrt{N_v}}{n_\ell^2}\Upsilon_{\mathrm{iO}}\right|^2 \left(\frac{c}{2\pi}|\sqrt{n_\ell}E_0|^2\right)^2, \\ I(2\omega) &= \frac{32\pi^3\omega^2}{c^3\cos^2\theta_0} \left|\frac{\sqrt{N_v}}{n_\ell^2}\Upsilon_{\mathrm{iO}}\right|^2 I^2(\omega), \\ \mathcal{R}_{\mathrm{iO}}(2\omega) &= \frac{32\pi^3\omega^2}{c^3\cos^2\theta_0} \left|\frac{1}{n_\ell}\Upsilon_{\mathrm{iO}}\right|^2, \end{aligned} \tag{2.42}$$

and in MKS units ($\eta = 1/2$)

$$\begin{aligned} |E(2\omega)|^2 &= |E_0|^4 \frac{\omega^2}{c^2 W_v^2} |\Upsilon_{\mathrm{iO}}|^2 \\ 2\epsilon_0 c|\sqrt{N_v}E(2\omega)|^2 &= \frac{2\epsilon_0\omega^2}{c\cos^2\theta_0} \left|\frac{\sqrt{N_v}}{n_\ell^2}\Upsilon_{\mathrm{iO}}\right|^2 \frac{1}{4\epsilon_0^2 c^2} \left(2\epsilon_0 c|\sqrt{n_\ell}E_0|^2\right)^2, \\ I(2\omega) &= \frac{\omega^2}{2\epsilon_0 c^3\cos^2\theta_0} \left|\frac{\sqrt{N_v}}{n_\ell^2}\Upsilon_{\mathrm{iO}}\right|^2 I^2(\omega), \\ \mathcal{R}_{\mathrm{iO}}(2\omega) &= \frac{\omega^2}{2\epsilon_0 c^3\cos^2\theta_0} \left|\frac{1}{n_\ell}\Upsilon_{\mathrm{iO}}\right|^2, \end{aligned} \tag{2.43}$$

$$\mathcal{R}_{\rm iO}(2\omega)\begin{cases}\frac{32\pi^3\omega^2}{c^3\cos^2\theta_0}\left|\frac{1}{n_\ell}\Upsilon_{\rm iO}\right|^2 & \text{(cgs units)}\\ \frac{\omega^2}{2\epsilon_0 c^3\cos^2\theta_0}\left|\frac{1}{n_\ell}\Upsilon_{\rm iO}\right|^2 & \text{(MKS units)}\end{cases}, \tag{2.44}$$

as the SHG yield, where $N_v = 1$ and $W_v = \cos\theta_0$. In the MKS unit system $\boldsymbol{\chi}$ is given in m^2/V, since it is a surface second order nonlinear susceptibility, and $\mathcal{R}_{\rm iO}$ is given in m^2/W.

`tal vez esto al apendice` At this point we mention that to recover the results of Ref. [25] which are equivalent of those of Ref. [27], we take $\mathbf{e}_\ell^{2\omega} \to \mathbf{e}_v^{2\omega}$, $\mathbf{e}_\ell^{\omega} \to \mathbf{e}_b^{\omega}$, and then

$$\mathcal{R}(2\omega) = \frac{32\pi^3\omega^2}{c^3\cos^2\theta_0}\left|\mathbf{e}_v^{2\omega}\cdot\boldsymbol{\chi}:\mathbf{e}_b^{\omega}\mathbf{e}_b^{\omega}\right|^2, \tag{2.45}$$

will give the SHG yield of a nonlinear polarization sheet radiating from vacuum on top of the surface and where the fundamental field is evaluated below the surface that is characterized by $\epsilon_b(\omega)$.

2.2 One SH Reflection

Therefore, the total radiated field at 2ω is

$$\begin{aligned}\mathbf{E}(2\omega) = {} & E_s(2\omega)\left(\mathbf{T}^{\ell v} + \mathbf{T}^{\ell v}\cdot\mathbf{R}^{\ell b}\right)\cdot\hat{\mathbf{s}}\\ & + E_{p+}(2\omega)\mathbf{T}^{\ell v}\cdot\hat{\mathbf{P}}_{\ell+} + E_{p-}(2\omega)\mathbf{T}^{\ell v}\cdot\mathbf{R}^{\ell b}\cdot\hat{\mathbf{P}}_{\ell-}.\end{aligned}$$

The first term is the transmitted s-polarized field, the second one is the reflected and then transmitted s-polarized field and the third and fourth terms are the equivalent fields for p-polarization. The transmission is from the layer into vacuum, and the reflection between the layer and the bulk. After some simple algebra, we obtain

$$\mathbf{E}(2\omega) = \frac{2\pi i\tilde{\Omega}}{K_\ell}\mathbf{H}_\ell\cdot\boldsymbol{\mathcal{P}}(2\omega), \tag{2.46}$$

where,

$$\mathbf{H}_\ell = \hat{\mathbf{s}}\,T_s^{\ell v}\left(1 + R_s^{\ell b}\right)\hat{\mathbf{s}} + \hat{\mathbf{P}}_{v+}T_p^{\ell v}\left(\hat{\mathbf{P}}_{\ell+} + R_p^{\ell b}\hat{\mathbf{P}}_{\ell-}\right). \tag{2.47}$$

2.3 $\mathcal{R}_{\rm iF}$ for different polarization cases

We obtain $\mathcal{R}_{\rm iF}$ from Eq. (2.44) for the most commonly used polarizations of incoming and outgoing fields, i.e., iF=pP, pS, sP or sS. For this, we have

to explicitely expand Υ_{iF} (Eq. (2.41)). First, by substituting Eqs. (2.7) and (2.8) into Eq. (2.34), we obtain

$$\mathbf{e}_\ell^{2\omega,\mathrm{P}} = \frac{T_p^{v\ell}}{N_\ell}\big(\sin\theta_0 R_p^{M+}\hat{\mathbf{z}} - W_\ell R_p^{M-}\cos\phi\hat{\mathbf{x}} - W_\ell R_p^{M-}\sin\phi\hat{\mathbf{y}}\big), \tag{2.48}$$

for P ($\hat{\mathbf{e}}^{\mathrm{F}} = \hat{\mathbf{P}}_{v+}$) outgoing polarization, and

$$\mathbf{e}_\ell^{2\omega,\mathrm{S}} = T_s^{v\ell} R_s^{M+}\left(-\sin\phi\hat{\mathbf{x}} + \cos\phi\hat{\mathbf{y}}\right). \tag{2.49}$$

for S ($\hat{\mathbf{e}}^{\mathrm{F}} = \hat{\mathbf{s}}$) outgoing polarization. Secondly, using again Eqs. (2.7) and (2.8), but now with Eq. (2.29), we obtain for p incoming polarization ($\hat{\mathbf{e}}^{\mathrm{i}} = \hat{\mathbf{p}}_{v-}$),

$$\mathbf{e}_\ell^{\omega,\mathrm{p}}\mathbf{e}_\ell^{\omega,\mathrm{p}} = \left(\frac{t_p^{v\ell}}{n_\ell}\right)^2\Big(\left(r_p^{M-}\right)^2 w_\ell^2\cos^2\phi\hat{\mathbf{x}}\hat{\mathbf{x}} + 2\left(r_p^{M-}\right)^2 w_\ell^2\sin\phi\cos\phi\hat{\mathbf{x}}\hat{\mathbf{y}} + 2r_p^{M+}r_p^{M-}w_\ell\sin\theta_0\cos\phi\hat{\mathbf{x}}\hat{\mathbf{z}}$$
$$+\left(r_p^{M-}\right)^2 w_\ell^2\sin^2\phi\hat{\mathbf{y}}\hat{\mathbf{y}} + 2r_p^{M+}r_p^{M-}w_\ell\sin\theta_0\sin\phi\hat{\mathbf{y}}\hat{\mathbf{z}} + \left(r_p^{M+}\right)^2\sin^2\theta_0\hat{\mathbf{z}}\hat{\mathbf{z}}\Big), \tag{2.50}$$

and with Eq. (**??**) for s incoming polarization ($\hat{\mathbf{e}}^{\mathrm{i}} = \hat{\mathbf{s}}$),

$$\mathbf{e}_\ell^{\omega,\mathrm{s}}\mathbf{e}_\ell^{\omega,\mathrm{s}} = \left(t_s^{v\ell}r_s^{M+}\right)^2\left(\sin^2\phi\hat{\mathbf{x}}\hat{\mathbf{x}} + \cos^2\phi\hat{\mathbf{y}}\hat{\mathbf{y}} - 2\sin\phi\cos\phi\hat{\mathbf{x}}\hat{\mathbf{y}}\right). \tag{2.51}$$

So to calculate $\mathcal{R}_{\mathrm{iF}}$, we summarize in Table 2.4 the combination of the equations needed for all four polarization cases. In the following subsections we write down the explicit expressions for Υ_{iF} for the most general case where the surface has no symmetry other than that of noncentrosymmetry. We then develop these expressions for particular cases of the most commonly investigated surfaces, the (111), (100), and (110) crystallographic faces. For ease of writing we split Υ_{iF} as

$$\Upsilon_{\mathrm{iF}} = \Gamma_{\mathrm{iF}}\, r_{\mathrm{iF}}, \tag{2.52}$$

and in Table 2.1 we list, for each surface, the components of $\boldsymbol{\chi}$ different from zero.[27, **?**]

2.3.1 $\mathcal{R}_{pP}$

Per Table 2.4, $\mathcal{R}_{pP}$ requires Eqs. (2.48) and (2.50). After some algebra, we obtain that

$$\Gamma_{pP} = \frac{T_p^{v\ell}}{N_\ell}\left(\frac{t_p^{v\ell}}{n_\ell}\right)^2, \tag{2.53}$$

(111)-C_{3v}	(110)-C_{2v}	(100)-C_{4v}
χ_{zzz}	χ_{zzz}	χ_{zzz}
$\chi_{zxx} = \chi_{zyy}$	$\chi_{zxx} \neq \chi_{zyy}$	$\chi_{zxx} = \chi_{zyy}$
$\chi_{xxz} = \chi_{yyz}$	$\chi_{xxz} \neq \chi_{yyz}$	$\chi_{xxz} = \chi_{yyz}$
$\chi_{xxx} = -\chi_{xyy} = -\chi_{yyx}$		

Table 2.1: Components of $\boldsymbol{\chi}$ for the (111), (110) and (100) crystallographic faces, belonging to the C_{3v}, C_{2v}, and C_{4v}, symmetry groups, respectively. For the (111) surface we choose the x and y axes along the $[11\bar{2}]$ and $[1\bar{1}0]$ directions, respectively. For the (110) and (100) we consider the y axis perpendicular to the plane of symmetry.[27] We remark that in general $\boldsymbol{\chi}^{(111)} \neq \boldsymbol{\chi}^{(110)} \neq \boldsymbol{\chi}^{(100)}$.

and

$$\begin{aligned} r_{pP} = &- R_p^{M-}\left(r_p^{M-}\right)^2 w_\ell^2 W_\ell \cos^3\phi\chi_{xxx} - 2R_p^{M-}\left(r_p^{M-}\right)^2 w_\ell^2 W_\ell \sin\phi\cos^2\phi\chi_{xxy} \\ &- 2R_p^{M-}r_p^{M+}r_p^{M-}w_\ell W_\ell \sin\theta_0\cos^2\phi\chi_{xxz} - R_p^{M-}\left(r_p^{M-}\right)^2 w_\ell^2 W_\ell \sin^2\phi\cos\phi\chi_{xyy} \\ &- 2R_p^{M-}r_p^{M+}r_p^{M-}w_\ell W_\ell \sin\theta_0\sin\phi\cos\phi\chi_{xyz} - R_p^{M-}\left(r_p^{M+}\right)^2 W_\ell \sin^2\theta_0\cos\phi\chi_{xzz} \\ &- R_p^{M-}\left(r_p^{M-}\right)^2 w_\ell^2 W_\ell \sin\phi\cos^2\phi\chi_{yxx} - 2R_p^{M-}\left(r_p^{M-}\right)^2 w_\ell^2 W_\ell \sin^2\phi\cos\phi\chi_{yxy} \\ &- 2R_p^{M-}r_p^{M+}r_p^{M-}w_\ell W_\ell \sin\theta_0\sin\phi\cos\phi\chi_{yxz} - R_p^{M-}\left(r_p^{M-}\right)^2 w_\ell^2 W_\ell \sin^3\phi\chi_{yyy} \\ &- 2R_p^{M-}r_p^{M+}r_p^{M-}w_\ell W_\ell \sin\theta_0\sin^2\phi\chi_{yyz} - R_p^{M-}\left(r_p^{M+}\right)^2 W_\ell \sin^2\theta_0\sin\phi\chi_{yzz} \\ &+ R_p^{M+}\left(r_p^{M-}\right)^2 w_\ell^2 \sin\theta_0\cos^2\phi\chi_{zxx} + 2R_p^{M+}r_p^{M+}r_p^{M-}w_\ell \sin^2\theta_0\cos\phi\chi_{zxz} \\ &+ 2R_p^{M+}\left(r_p^{M-}\right)^2 w_\ell^2 \sin\theta_0\sin\phi\cos\phi\chi_{zxy} + R_p^{M+}\left(r_p^{M-}\right)^2 w_\ell^2 \sin\theta_0\sin^2\phi\chi_{zyy} \\ &+ 2R_p^{M+}r_p^{M+}r_p^{M-}w_\ell \sin^2\theta_0\sin\phi\chi_{zzy} + R_p^{M+}\left(r_p^{M+}\right)^2 \sin^3\theta_0\chi_{zzz}, \end{aligned} \tag{2.54}$$

Case	$\hat{\mathbf{e}}^{\mathrm{F}}$	$\hat{\mathbf{e}}^{\mathrm{i}}$	$\mathbf{e}_\ell^{2\omega,\mathrm{F}}$	$\mathbf{e}_\ell^{\omega,\mathrm{i}}\mathbf{e}_\ell^{\omega,\mathrm{i}}$
$\mathcal{R}_{pP}$	$\hat{\mathbf{P}}_{v+}$	$\hat{\mathbf{p}}_{v-}$	Eq. (2.48)	Eq. (2.50)
$\mathcal{R}_{pS}$	$\hat{\mathbf{S}}$	$\hat{\mathbf{p}}_{v-}$	Eq. (2.49)	Eq. (2.50)
$\mathcal{R}_{sP}$	$\hat{\mathbf{P}}_{v+}$	$\hat{\mathbf{s}}$	Eq. (2.48)	Eq. (2.51)
$\mathcal{R}_{sS}$	$\hat{\mathbf{S}}$	$\hat{\mathbf{s}}$	Eq. (2.49)	Eq. (2.51)

Table 2.2: Polarization unit vectors for $\hat{\mathbf{e}}^{\mathrm{F}}$ and $\hat{\mathbf{e}}^{\mathrm{i}}$, and equations describing $\mathbf{e}_\ell^{2\omega,\mathrm{F}}$ and $\mathbf{e}_\ell^{\omega,\mathrm{i}}\mathbf{e}_\ell^{\omega,\mathrm{i}}$ for each polarization case.

where all 18 independent components of $\boldsymbol{\chi}$ valid for a surface with no symmetries contribute to $\mathcal{R}_{pP}$. Recall that $\chi_{ijk} = \chi_{ikj}$. Using Table 2.1, we present the expressions for each of the three surfaces being considered here. For the (111) surface we obtain

$$\begin{aligned} r_{pP}^{(111)} &= R_p^{M+}\sin\theta_0\Big(\left(r_p^{M+}\right)^2\sin^2\theta_0\chi_{zzz} + \left(r_p^{M-}\right)^2 w_\ell^2\chi_{zxx}\Big) \\ &\quad - R_p^{M-}w_\ell W_\ell\Big(2r_p^{M+}r_p^{M-}\sin\theta_0\chi_{xxz} + \left(r_p^{M-}\right)^2 w_\ell\chi_{xxx}\cos 3\phi\Big), \end{aligned} \tag{2.55}$$

where the three-fold azimuthal symmetry of the SHG signal, typical of the C_{3v} symmetry group, is seen in the 3ϕ argument of the cosine function. For the (110) we have that

$$\begin{aligned} r_{pP}^{(110)} &= R_p^{M+}\sin\theta_0\Bigg(\left(r_p^{M+}\right)^2\sin^2\theta_0\chi_{zzz} + \left(r_p^{M-}\right)^2 w_\ell^2\left(\frac{\chi_{zyy}+\chi_{zxx}}{2} + \frac{\chi_{zyy}-\chi_{zxx}}{2}\cos 2\phi\right)\Bigg) \\ &\quad - 2R_p^{M-}r_p^{M+}r_p^{M-}w_\ell W_\ell\sin\theta_0\left(\frac{\chi_{yyz}+\chi_{xxz}}{2} + \frac{\chi_{yyz}-\chi_{xxz}}{2}\cos 2\phi\right). \end{aligned} \tag{2.56}$$

The two-fold azimuthal symmetry of the SHG signal, typical of the C_{2v} symmetry group, is seen in the 2ϕ argument of the cosine function. For the (100) surface we simply make $\chi_{zxx} = \chi_{zyy}$ and $\chi_{xxz} = \chi_{yyz}$, as seen from Table 2.1, and above expression reduces to

$$r_{pP}^{(100)} = R_p^{M+}\sin\theta_0\Big(\left(r_p^{M+}\right)^2\sin^2\theta_0\chi_{zzz} + \left(r_p^{M-}\right)^2 w_\ell^2\chi_{zxx}\Big) - 2R_p^{M-}r_p^{M+}r_p^{M-}w_\ell W_\ell\sin\theta_0\chi_{xxz}. \tag{2.57}$$

where we mention that the azimutal 4ϕ symmetry for the C_{4v} group of the (100) surface is absent in above expresion since such contribution is only related to the bulk nonlinear quadrupolar SH term,[27] that is neglected in this work.

2.3.2 $\mathcal{R}_{pS}$

Per Table 2.4, $\mathcal{R}_{pS}$ requires Eqs. (2.49) and (2.50). After some algebra, we obtain that

$$\Gamma_{pS} = T_s^{v\ell}R_s^{M+}\left(\frac{t_p^{v\ell}}{n_\ell}\right)^2, \tag{2.58}$$

and

$$\begin{aligned} r_{pS} = &- \left(r_p^{M-}\right)^2 w_\ell^2 \sin\phi\cos^2\phi\chi_{xxx} - 2\left(r_p^{M-}\right)^2 w_\ell^2 \sin^2\phi\cos\phi\chi_{xxy} - 2r_p^{M+}r_p^{M-}w_\ell \sin\theta_0 \sin\phi\cos\phi \\ &- \left(r_p^{M-}\right)^2 w_\ell^2 \sin^3\phi\chi_{xyy} - 2r_p^{M+}r_p^{M-}w_\ell \sin\theta_0 \sin^2\phi\chi_{xzy} - \left(r_p^{M+}\right)^2 \sin^2\theta_0 \sin\phi\chi_{xzz} \\ &+ \left(r_p^{M-}\right)^2 w_\ell^2 \cos^3\phi\chi_{yxx} + 2\left(r_p^{M-}\right)^2 w_\ell^2 \sin\phi\cos^2\phi\chi_{yxy} + 2r_p^{M+}r_p^{M-}w_\ell \sin\theta_0 \cos^2\phi\chi_{yxz} \\ &+ \left(r_p^{M-}\right)^2 w_\ell^2 \sin^2\phi\cos\phi\chi_{yyy} + 2r_p^{M+}r_p^{M-}w_\ell \sin\theta_0 \sin\phi\cos\phi\chi_{yzy} + \left(r_p^{M+}\right)^2 \sin^2\theta_0 \cos\phi\chi_{yzz} \end{aligned} \tag{2.59}$$

In this case 12 out of the 18 components of $\boldsymbol{\chi}$ valid for a surface with no symmetries, contribute to $\mathcal{R}_{pS}$. This is so, because there is no $\mathcal{P}_z$ component, as the outgoing polarization is S. From Table 2.1 we obtain,

$$r_{pS}^{(111)} = -\left(r_p^{M-}\right)^2 w_\ell^2 \chi_{xxx} \sin 3\phi, \tag{2.60}$$

for the (111) surface,

$$r_{sP}^{(110)} = r_p^{M+}r_p^{M-}w_\ell \sin\theta_0(\chi_{yyz} - \chi_{xxz}) \sin 2\phi, \tag{2.61}$$

for the (110) surface, finally,

$$r_{pS}^{(100)} = 0, \tag{2.62}$$

for the (100) surface, where again, the zero value is only surface related as we neglect the bulk nonlinear quadrupolar contribution.

2.3.3 $\mathcal{R}_{sP}$

Per Table 2.4, $\mathcal{R}_{sP}$ requires Eqs. (2.48) and (2.51). After some algebra, we obtain that

$$\Gamma_{sP} = \frac{T_p^{v\ell}}{N_\ell}\left(t_s^{v\ell}r_s^{M+}\right)^2, \tag{2.63}$$

and

$$\begin{aligned} r_{sP} = &R_p^{M-}W_\ell\big(-\sin^2\phi\cos\phi\chi_{xxx} + 2\sin\phi\cos^2\phi\chi_{xxy} - \cos^3\phi\chi_{xyy}\big) \\ &R_p^{M-}W_\ell\big(-\sin^3\phi\chi_{yxx} + 2\sin^2\phi\cos\phi\chi_{yxy} - \sin\phi\cos^2\phi\chi_{yyy}\big) \\ &R_p^{M+}\sin\theta_0\big(\sin^2\phi\chi_{zxx} - 2\sin\phi\cos\phi\chi_{zxy} + \cos^2\phi\chi_{zyy}\big). \end{aligned} \tag{2.64}$$

In this case 9 out of the 18 components of $\boldsymbol{\chi}(2\omega)$ valid for a surface with no symmetries, contribute to $\mathcal{R}_{sP}$. This is so, because there is no $E_z(\omega)$ component, as the incoming polarization is s. From Table 2.1 we get,

$$r_{sP}^{(111)} = R_p^{M+}\sin\theta_0\chi_{zxx} + R_p^{M-}W_\ell\chi_{xxx}\cos 3\phi, \tag{2.65}$$

for the (111) surface,

$$r_{sP}^{(110)} = R_p^{M+} \sin\theta_0 \left(\frac{\chi_{zxx} + \chi_{zyy}}{2} + \frac{\chi_{zyy} - \chi_{zxx}}{2} \cos 2\phi \right), \tag{2.66}$$

for the (110) surface, and

$$r_{sP}^{(100)} = R_p^{M+} \sin\theta_0 \chi_{zxx}, \tag{2.67}$$

for the (100) surface.

2.3.4 $\mathcal{R}_{sS}$

Per Table 2.4, $\mathcal{R}_{sS}$ requires Eqs. (2.49) and (2.51). After some algebra, we obtain that

$$\Gamma_{sS} = T_s^{v\ell} R_s^{M+} \left(t_s^{v\ell} r_s^{M+} \right)^2, \tag{2.68}$$

and

$$\begin{aligned} r_{sS} = &- \sin^3\phi \chi_{xxx} + 2\sin^2\phi\cos\phi\chi_{xxy} - \sin\phi\cos^2\phi\chi_{xyy} \\ &+ \sin^2\phi\cos\phi\chi_{yxx} + \cos^3\phi\chi_{yyy} - 2\sin\phi\cos^2\phi\chi_{yxy}. \end{aligned} \tag{2.69}$$

In this case 6 out of the 18 components of $\boldsymbol{\chi}(2\omega)$ valid for a surface with no symmetries, contribute to $\mathcal{R}_{sS}$. This is so, because there is neither an $E_z(\omega)$ component, as the incoming polarization is s, nor a $\sqrt{}^z$ component, as the outgoing polarization is S. From Table 2.1, we get

$$r_{sS}^{(111)} = \chi_{xxx} \sin 3\phi, \tag{2.70}$$

for the (111) surface,

$$r_{sS}^{(110)} = 0, \tag{2.71}$$

and

$$r_{sS}^{(100)} = 0, \tag{2.72}$$

for the (110) and (100) surfaces, respectively, both being zero as the bulk nonlinear quadrupolar contribution is not considered here.

2.4 Different scenarios

In this section we present five different scenarios, alternative to the three-layer model presented above, for the placement of the nonlinear polarization $\boldsymbol{\mathcal{P}}(2\omega)$ and the fundamental electric field $\mathbf{E}(\omega)$. In these scenarios we neglect the SH multiple reflections contained in $R_l^{M\pm}$ through R_l^M, Eq. (2.32) and (2.23), respectively, for which we take $R_l^M \to R_l^{\ell b}$. This is equivalent of taking only one single reflection from the ℓb interface. Within the three-layer model we neglect multiple reflections, as yet another scenario, by the same $R_l^M \to R_l^{\ell b}$ replacement in the formulae shown in the previous section. In what follows, we confine ourselves only to the the (111) surface and the pP combination of incoming-outgoing polarizations, since this is the case where the proposed scenarios differ the most. However, the other pS, sP and sS polarization cases, and (100) and (110) surfaces could be worked out along the same lines described below. For all the scenarios we have that the omission of multiple SH reflections by taking $R_p^{M\pm} \to 1 \pm R_p^{\ell b}$ (Eq. (2.32)) reduces to

$$\begin{aligned} R_p^{M+} &\to \frac{N_b}{N_\ell} T_p^{\ell b} \\ R_p^{M-} &\to \frac{N_\ell}{N_b}\frac{W_b}{W_\ell} T_p^{\ell b}, \end{aligned} \tag{2.73}$$

after using the expressions in Eq. (2.14).

2.4.1 Three layer model: without multiple reflections

Using Eq. (2.73) in Eq. (2.55) we obtain

$$\Gamma_{pP} = \frac{T_p^{\ell v} T_p^{\ell b}}{N_\ell^2 N_b} \left(\frac{t_p^{v\ell} t_p^{\ell b}}{n_\ell^2 n_b} \right)^2, \tag{2.74}$$

and

$$r_{pP}^{(111)} = N_b^2 \sin\theta_0 \Big(n_b^4 \sin^2\theta_0 \chi_{zzz} + n_\ell^4 w_b^2 \chi_{zxx} \Big) - N_\ell^2 n_\ell^2 w_b W_b \Big(2 n_b^2 \sin\theta_0 \chi_{xxz} + n_\ell^2 w_b \chi_{xxx} \cos(3\phi) \Big). \tag{2.75}$$

Now that we have neglected multiple SH reflections, we can use above two expressions for Γ_{pP} and r_{pP} to obtain the following four scenarios, by using the choices as described in each subsection bellow. We mention that by neglecting the multiple reflections the thickness d of layer ℓ disappears from the formulation, and the location of the nonlinear polarization sheet $\mathbf{P}(\mathbf{r}, t)$ (Eq. (2.3)) at d_2 (see Fig. **??**), is inmaterial.

2.4.2 Two layer model

Historically, this is the model most used in the literature, and our three-layer model with multiple reflections, as mentioned in the introduction, is a clear improvement upon the simple two layer model. In the two layer model, one considers that $\boldsymbol{\mathcal{P}}(2\omega)$, is evaluated in the vacuum region, while the fundamental fields are evaluated in the bulk region.[27, 25] To do this, we take the 2ω radiations factors for vacuum by taking $\ell = v$, thus $\epsilon_\ell(2\omega) = 1$, $T_p^{\ell v} = 1$, $T_p^{\ell b} = T_p^{vb}$, and the fundamental field inside medium b by taking $\ell = b$, thus $\epsilon_\ell(\omega) = \epsilon_b(\omega)$, $t_p^{v\ell} = t_p^{vb}$, and $t_p^{\ell b} = 1$. With these choices Eqs. (2.74) and (2.75) reduce to

$$\Gamma_{pP} = \frac{T_p^{vb}(t_p^{vb})^2}{n_b^2 N_b}, \tag{2.76}$$

and

$$r_{pP}^{(111)} = N_b^2 \sin\theta_0 \Big(\sin^2\theta_0 \chi_{zzz} + w_b^2 \chi_{zxx} \Big) - w_b W_b \Big(2\sin\theta_0 \chi_{xxz} + w_b \chi_{xxx} \cos(3\phi) \Big), \tag{2.77}$$

and these expressions are in agreement with Refs. [27] and [25].

2.4.3 Taking the nonlinear polarization and the fundamental fields in the bulk

We follow the same procedure as above considering that both the 2ω and 1ω terms will be evaluated in the bulk taking $\ell = b$, thus $\epsilon_\ell(2\omega) = \epsilon_b(2\omega)$, $T_p^{v\ell} = T_p^{vb}$, $T_p^{\ell b} = 1$, and $\epsilon_\ell(\omega) = \epsilon_b(\omega)$, $t_p^{v\ell} = t_p^{vb}$, and $t_p^{\ell b} = 1$. With these choices Eqs. (2.74) and (2.75) reduce to

$$\Gamma_{pP} = \frac{T_p^{vb}\left(t_p^{vb}\right)^2}{n_b^2 N_b}, \tag{2.78}$$

and

$$r_{pP}^{(111)} = \sin^3\theta_0 \chi_{zzz} + w_b^2 \sin\theta_0 \chi_{zxx} - 2 w_b W_b \sin\theta_0 \chi_{xxz} - w_b^2 W_b \chi_{xxx} \cos 3\phi. \tag{2.79}$$

2.4.4 Taking the nonlinear polarization in ℓ and the fundamental fields in the bulk

Again, we follow the same procedure as above considering that 2ω terms are evaluated in the thin layer ℓ, and the 1ω terms will be evaluated in the

Label	$\boldsymbol{\mathcal{P}}(2\omega)$	$\mathbf{E}(\omega)$
Three layer	ℓ	ℓ
Two layer	v	b
Bulk	b	b
Hybrid	ℓ	b
Vacuum	v	v

Table 2.3: Summary of SSHG yield models. "Label" is the name used in subsequent figures, while the remaining columns show in which medium we will consider the specified quantity. ℓ is the thin layer below the surface of the material, v is the vacuum region, and b is the bulk region of the material.

bulk by taking $\ell = b$, thus $\epsilon_\ell(\omega) = \epsilon_b(\omega)$, $t_p^{v\ell} = t_p^{vb}$, and $t_p^{\ell b} = 1$. With these choices Eqs. (2.74) and (2.75) reduce to

$$\Gamma_{pP}^{\ell b} = \frac{T_p^{v\ell} T_p^{\ell b} \left(t_p^{vb}\right)^2}{N_\ell^2 n_b^2 N_b}, \tag{2.80}$$

and

$$r_{pP}^{(111)} = N_b^2 \sin^3\theta_0 \chi_{zzz} + N_b^2 k_b^2 \sin\theta_0 \chi_{zxx} - 2N_\ell^2 w_b W_b \sin\theta_0 \chi_{xxz} - N_\ell^2 w_b^2 W_b \chi_{xxx} \cos 3\phi. \tag{2.81}$$

2.4.5 Taking the nonlinear polarization and the fundamental fields in the vacuum

Our last scenario considers both the $\boldsymbol{\mathcal{P}}(2\omega)$ and fundamental fields evaluated in the vacuum. We take $\ell = v$, thus $\epsilon_\ell(2\omega) = 1$, $T_p^{\ell v} = 1$, $T_p^{\ell b} = T_p^{vb}$, and $\epsilon_\ell(\omega) = 1$, $t_p^{v\ell} = 1$, and $t_p^{\ell b} = t_p^{vb}$. With these choices Eqs. (2.74) and (2.75) reduce to

$$\Gamma_{pP} = \frac{T_p^{vb} \left(t_p^{vb}\right)^2}{n_b^2 N_b}, \tag{2.82}$$

and

$$r_{pP}^{(111)} = n_b^4 N_b^2 \sin^3\theta_0 \chi_{zzz} + N_b^2 w_b^2 \sin\theta_0 \chi_{zxx} - 2n_b^2 w_b W_b \sin\theta_0 \chi_{xxz} - w_b^2 W_b \chi_{xxx} \cos 3\phi. \tag{2.83}$$

We summarize all these scenarios in Table 2.3 for quick reference.

2.4.6 Summary

We present the final expressions for each polarization case in Table 2.4.

iF	Γ_{iF}^{ℓ}	r_{iF}^{ℓ}
pP	$\frac{T_p^{v\ell}}{N_\ell}\left(\frac{t_p^{v\ell}t_p^{\ell b}}{n_\ell^2 n_b}\right)^2$	$R_p^{M+}\sin\theta_0(n_b^4\sin^2\theta_0\chi_{zzz}+n_\ell^4 w_b^2\chi_{zxx})$ $-\quad R_p^{M-}n_\ell^2 w_b W_\ell(2n_b^2\sin\theta_0\chi_{xxz}\quad+$ $n_\ell^2 w_b\chi_{xxx}\cos 3\phi)$
pS	$T_s^{v\ell}R_s^{M+}\left(\frac{t_p^{v\ell}t_p^{\ell b}}{n_\ell^2 n_b}\right)^2$	$-n_\ell^4 w_b^2\chi_{xxx}\sin 3\phi$
sP	$\frac{T_p^{v\ell}}{N_\ell}\left(t_s^{v\ell}t_s^{\ell b}\right)^2$	$R_p^{M+}\sin\theta_0\chi_{zxx}+R_p^{M-}W_\ell\chi_{xxx}\cos 3\phi$
sS	$T_s^{v\ell}R_s^{M+}\left(t_s^{v\ell}t_s^{\ell b}\right)^2$	$\chi_{xxx}\sin 3\phi$

Table 2.4: The expressions needed to calculate the SHG yield for the (111) surface, for each polarization case.

Bibliography

[1] M. C. Downer, B. S. Mendoza, and V. I. Gavrilenko. Optical second harmonic spectroscopy of semiconductor surfaces: advances in microscopic understanding. *Surf. Interface Anal.*, 31(10):966–986, 2001.

[2] C. Aversa and J. E. Sipe. Nonlinear optical susceptibilities of semiconductors: Results with a length-gauge analysis. *Phys. Rev. B*, 52(20):14636–14645, 1995.

[3] J. E. Sipe and A. I. Shkrebtii. Second-order optical response in semiconductors. *Phys. Rev. B*, 61(8):5337, 2000.

[4] W. R. L. Lambrecht and S. N. Rashkeev. From band structures to linear and nonlinear optical spectra in semiconductors. *Phys. Status Solidi B*, 217(1):599–640, 2000.

[5] E. N. Adams. The crystal momentum as a quantum mechanical operator. *J. Chem. Phys.*, 21(11):2013–2017, November 1953.

[6] E. I. Blount, F. Seitz, and D. Turnbull. Formalisms of band theory. *Solid State Phys.*, 13:305, 1962.

[7] S. Ismail-Beigi, E. K. Chang, and S. G. Louie. Coupling of nonlocal potentials to electromagnetic fields. *Phys. Rev. Lett.*, 87(8):087402, August 2001.

[8] C. Motta, M. Giantomassi, M. Cazzaniga, K. Gaál-Nagy, and X. Gonze. Implementation of techniques for computing optical properties in 0-3 dimensions, including a real-space cutoff, in ABINIT. *Comput. Mater. Sci.*, 50(2):698–703, 2010.

[9] L. Kleinman and D. M. Bylander. Efficacious form for model pseudopotentials. *Phys. Rev. Lett.*, 48(20):1425–1428, 1982.

[10] B. Adolph, V. I. Gavrilenko, K. Tenelsen, F. Bechstedt, and R. Del Sole. Nonlocality and many-body effects in the optical properties of semiconductors. *Phys. Rev. B*, 53(15):9797–9808, 1996.

[11] L. Reining, R. Del Sole, M. Cini, and J. G. Ping. Microscopic calculation of second-harmonic generation at semiconductor surfaces: As/Si(111) as a test case. *Phys. Rev. B*, 50(12):8411–8422, 1994.

[12] B. S. Mendoza, A. Gaggiotti, and R. Del Sole. Microscopic theory of second harmonic generation at si (100) surfaces. *Phys. Rev. Lett.*, 81(17):3781–3784, 1998.

[13] B. S. Mendoza, M. Palummo, G. Onida, and R. Del Sole. Ab initio calculation of second-harmonic-generation at the si(100) surface. *Phys. Rev. B*, 63(20):205406, 2001.

[14] H. Sano, G. Mizutani, W. Wolf, and R. Podloucky. Ab initio study of linear and nonlinear optical responses of si(111) surfaces. *Phys. Rev. B*, 66(19):195338, November 2002.

[15] J. E. Mejía, B. S. Mendoza, and C. Salazar. Layer-by-layer analysis of second harmonic generation at a simple surface. *Revista Mexicana de Física*, 50(2):134–139, 2004.

[16] C. Hogan, R. Del Sole, and G. Onida. Optical properties of real surfaces from microscopic calculations of the dielectric function of finite atomic slabs. *Phys. Rev. B*, 68(3):035405, 2003.

[17] C. Castillo, B. S. Mendoza, W. G. Schmidt, P. H. Hahn, and F. Bechstedt. Layer-by-layer analysis of surface reflectance anisotropy in semiconductors. *Phys. Rev. B*, 68(4):041310, 2003.

[18] B. S. Mendoza, F. Nastos, N. Arzate, and J. Sipe. Layer-by-layer analysis of the linear optical response of clean and hydrogenated si(100) surfaces. *Phys. Rev. B*, 74(7):075318, 2006.

[19] Nicolas Tancogne-Dejean private communication. Indeed, one can compute the layered contribution of the non-local contribution to $\mathbf{v}$ with an analytic expression. However, one needs to compute this within the DP code.

[20] S. N. Rashkeev, W. R. L. Lambrecht, and B. Segall. Efficient ab initio method for the calculation of frequency-dependent second-order optical response in semiconductors. *Phys. Rev. B*, 57(7):3905–3919, 1998.

[21] Valérie Véniard, E. Luppi, and H. Hübener. unpublished.

[22] Neil W. Ashcroft and N. David Mermin. *Solid State Physics*. Saunders College, Philadelphia, 1976.

[23] Robert W. Boyd. *Nonlinear Optics*. AP, New York, 2007.

[24] Michele Cini. Simple model of electric-dipole second-harmonic generation from interfaces. *Phys. Rev. B*, 43(6):4792–4802, February 1991.

[25] V. Mizrahi and J. E. Sipe. Phenomenological treatment of surface second-harmonic generation. *J. Opt. Soc. Am. B*, 5(3):660–667, 1988.

[26] J. E. Sipe. New Green-function formalism for surface optics. *Journal of the Optical Society of America B*, 4(4):481–489, 1987.

[27] J. E. Sipe, D. J. Moss, and H. M. van Driel. Phenomenological theory of optical second- and third-harmonic generation from cubic centrosymmetric crystals. *Phys. Rev. B*, 35(3):1129–1141, January 1987.